HARDWARE ACCELERATION OF SIMILARITY QUERIES USING GRAPHIC PROCESSOR UNITS

A THESIS

SUBMITTED TO THE DEPARTMENT OF COMPUTER ENGINEERING

AND THE INSTITUTE OF ENGINEERING AND SCIENCE

OF BILKENT UNIVERSITY

IN PARTIAL FULFILLMENT OF THE REQUIREMENTS

FOR THE DEGREE OF

MASTER OF SCIENCE

By

Atilla Genç

January, 2010

I certify that I have read this thesis and that in my opinion it is fully adequate, in scope and in quality, as a thesis for the degree of Master of Science.

Asst. Prof. Dr. İbrahim Körpeoğlu(Supervisor)

I certify that I have read this thesis and that in my opinion it is fully adequate, in scope and in quality, as a thesis for the degree of Master of Science.

Dr. Cengiz Çelik(Co-Supervisor)

I certify that I have read this thesis and that in my opinion it is fully adequate, in scope and in quality, as a thesis for the degree of Master of Science.

Asst.Prof. Ali Aydın Selçuk

I certify that I have read this thesis and that in my opinion it is fully adequate, in scope and in quality, as a thesis for the degree of Master of Science.

Asst.Prof. Özcan Öztürk

I certify that I have read this thesis and that in my opinion it is fully adequate, in scope and in quality, as a thesis for the degree of Master of Science.

Asst.Prof. Tansel Özyer

Approved for the Institute of Engineering and Science:

Prof. Dr. Mehmet B. Baray
Director of the Institute

ABSTRACT

HARDWARE ACCELERATION OF SIMILARITY QUERIES USING GRAPHIC PROCESSOR UNITS

Atilla Genç
M.S. in Computer Engineering
Supervisor: Asst. Prof. Dr. İbrahim Körpeoğlu
Co-Supervisor: Dr. Cengiz Çelik
January, 2010

A Graphic Processing Unit (GPU) is primarily designed for real-time rendering. In contrast to a Central Processing Unit (CPU) that have complex instructions and a limited number of pipelines, a GPU has simpler instructions and many execution pipelines to process vector data in a massively parallel fashion. In addition to its regular tasks, GPU instruction set can be used for performing other types of general-purpose computations as well. Several frameworks like Brook+, ATI CAL, OpenCL, and Nvidia Cuda have been proposed to utilize computational power of the GPU in general computing. This has provided interest and opportunities for accelerating different types of applications.

This thesis explores ways of taking advantage of the GPU in the field of metric space-based similarity searching. The KVP index structure has a simple organization that lends itself to be easily processed in parallel, in contrast to tree-based structures that requires frequent "pointer chasing" operations. Several implementations using the general purpose GPU programming frameworks (Brook+, ATI CAL and OpenCL) based on the ATI platform are provided. Experimental results of these implementations show that the GPU versions presented in this work are several times faster than the CPU versions.

Keywords: Similarity Search, General Purpose Computing on Graphic Processing Units, GPGPU.

ÖZET

GRAFİK İŞLEMCİ BİRİMLERİ KULLANILARAK BENZERLİK SORGULARININ HIZLANDIRILMASI

Atilla Genç
Bilgisayar Mühendisliği, Yüksek Lisans
Tez Yöneticisi: Asst. Prof. Dr. İbrahim Körpeoğlu
Tez Yöneticisi: Dr. Cengiz Çelik
Ocak, 2010

Grafik İşleme Birimi (GPU) birincil olarak gerçek zamanlı görüntü oluşturmak için tasarlanmıştır. Karmaşık komut kümesi ve sınırlı ardışık düzene sahip merkezi işlem biriminin aksine GPU daha basit bir komut kümesine ve vektör verilerini koşut olarak çalıştırabilecek çok sayıda yürütme ardışık düzenine sahiptir. Olağan görevlerine ek olarak, GPU komut kümesi başka tip genel amaçlı hesaplamalar için kullanılabilir. GPU'ların işlem gücünü genel amaçlı hesaplamalarda değerlendirebilmek için Brook+, ATI CAL, OpenCL ve Nvidia Cuda gibi değişik programlama çerçeve modelleri önerilmiştir. Bu durum pek çok uygulamanın hızlandırılması için fırsat doğurmuştur.

Bu çalışmada metrik tabanlı benzerlik araması alanında grafik kartlarının sağladığı avantajların kullanılması incelenmektedir. Sıkça "imleç takibi" gerektiren ağaç temelli yapıların aksine, KVP yapısı basit organizasyonu nedeniyle kolayca koşut olarak işlenmeye uygundur. ATI platformunda değişik genel amaçlı GPU programlama çerçeve modelleri kullanılarak (Brook+, ATI CAL ve OpenCL) Brute Force Linear Scan ve KVP algoritmaları gerçekleştirilmiş, yapılan çalışma sunulmuştur. Bu gerçekleştirimlerin deneysel sonuları GPU uygulamalarının CPU sürümlerinden çok daha hızlı olduğunu göstermektedir.

Anahtar sözcükler: Benzerlik Araması, Grafik İşleme Ünitelerinde Genel Amaçlı Hesaplama, GPGPU.

Acknowledgement

I would like to thank my supervisors, Asst. Prof. Dr. İbrahim Körpeoğlu and Dr. Cengiz Çelik for their guidance throughout my study.

Contents

List of Figures

List of Tables

Chapter 1

Introduction

A very important issue on any kind of data management is searching. Traditional database systems efficiently search for structured records. However, the new data types like image, video, audio, protein structures etc. are not very structured and can not be handled efficiently. In these cases, the similarity search paradigm is a better solution. Similarity searching consists of retrieving data that are similar to a given query. The measure of similarity is specifically defined with respect to the target application.

One popular approach for similarity searching is mapping database objects into feature vectors, which introduces an undesirable element of indirection into the process. A more direct approach is to define a distance function directly between objects. Typically such a function is taken from a metric space, which satisfies a number of properties, such as the triangle inequality. Index structures that can work for metric spaces have been reported to outperform vector-based counterparts in many applications. Metric spaces also provide a more general framework, such as defining a distance between objects can be accomplished more intuitively than mapping objects to feature vectors for some domains.

Downside of using metric distance functions for similarity search is that they are usually computationally expensive. As computers find usage in new areas, new applications with complex similarity measures comes on demand, causing an

urgent need to improve the efficiency of similarity queries. Index structures that are designed for similarity search seek to reduce the number of distance computations required to process a similarity search query. Another way of increasing speed of this expensive task is to find faster and more suitable configurations.

Recent graphics architectures provide tremendous memory bandwidth and computational horsepower. Their arithmetic power results from a highly specialized architecture, evolved and tuned over years to extract maximum performance on the highly parallel tasks of traditional computer graphics. Also early GPUs were fixed-function pipelines whose output was limited to 8-bit-per-channel color values, whereas modern GPUs now include fully programmable processing units that support vectorized floating-point operations. The increasing flexibility of GPUs, coupled with some creative uses of that flexibility by GPGPU developers, has enabled many applications outside the original narrow tasks for which GPUs were originally designed. Researchers and developers have become interested in utilizing this power for general-purpose computing, an effort known collectively as GPGPU (for General-Purpose computing on the GPU). Thus these advances on graphic cards suggest it to be a viable and cheap opportunity for a faster computational hardware.

Objective of this thesis is to explore ways of taking advantage of the advances in GPU architectures in the field of similarity searching by accelerating execution times; specifically in brute force linear scan technique and KVP algorithm.

This thesis is organized as follows. Chapter 2 gives a broad survey on similarity searching and has a section specifically for discussions of KVP algorithm that will be implemented. Chapter 3 gives a broad survey on general purpose computation on graphical cards. In chapter, 4 implementation details of similarity search algorithms are presented. Chapter 5 reports experimental results obtained by measuring execution times of implementations in CPU and GPU environments through a set of tests. Finally, in chapter 5 concluding remarks are presented.

Chapter 2

Similarity Search

2.1 Overview

One of the areas that computer systems had significant success is storage and retrieval of vast amounts of information. Many applications in computer science depend on efficient storage and retrieval of data. If data to be stored has some predefined structure, classical database methods that are designed to handle data objects provide quite a good performance. This predefined structure can be captured by treating the various attributes associated with the objects as records and these records can be stored in the database using some appropriate model like relational, object-oriented, object-relational,hierarchical, network, etc. The retrieval process, responding to queries like exact match, range, and join applied to some or all of the attributes, is then facilitated by building indexes on the relevant attributes. As mentioned before these techniques assume some predefined structure and more importantly, concepts like data equality and similarity are well defined and evaluation of equality and similarity are not very costly.

As the proliferation of computer systems in data management increase, new demands on data storage and management arise. Recent applications require management of larger data as well as storage and retrieval of data which has considerably less structure. A few examples of such data and applications of the

similarity search include: audio and image databases [21], video,audio recordings, text documents, time series, DNA sequences, fingerprints [59], face recognition [58] etc. Such data objects sometimes can be described via a set of features, which is called a feature vector. Feature vectors consists of features which are scalar values. For example, in the case of image data, the feature vector might include color, color moments, textures, or RGB values of the image pixels etc. which are scalar values. In the case of text documents, we might have one dimension per word, which can lead to prohibitively high dimensions. Also there are some cases where, even a feature vector may not be available. Sometimes we only have a set of objects and a distance function d, which is usually quite expensive to compute, where d specifies the degree of similarity (or dissimilarity) between all pairs of objects. The challenge with these kind of data is that usually the data can not be ordered and most of the time it is not meaningful to perform equality comparisons on it. To illustrate the point, consider retrieval of songs that are similar to a query song from a set of songs, or finding a images which contain a certain person from a set of images. When dealing with cases where data can not be sorted, nor a clear definition of equality or similarity can be provided, proximity becomes more appropriate retrieval criterion and queries can be defined as:

1. Finding objects whose feature values fall within a given range or where the distance, using a suitably defined distance metric, from some query object falls into a certain range (range queries).

2. Finding objects whose features have values similar to those of a given query object or set of query objects (nearest neighbor queries). In order to reduce the complexity of the search process, the precision of the required similarity can be an approximation (approximate nearest neighbor queries).

3. Finding pairs of objects from the same set or different sets which are sufficiently similar to each other (closest pairs queries).

The process of computing results to these queries is termed similarity searching.

The main problem with processing similarity search queries is the difficulty with dealing very large dimensions and cost of evaluating distance functions which are usually expensive to compute. Thus a good indexing method should be able to deal with high dimensions of data and/or reduce the number of distance computations to evaluate query.

If data can be modeled by feature vectors one can form indexes on various features as in the case of structured data and use point access methods (eg., [24, 77, 78]). These feature vectors are represented as coordinate vectors. In these approaches, it is assumed that the objects can be decomposed into or represented as vectors over some multi-dimensional space, and distances are measured using geometric distance functions like standard Euclidean distance. Numerous index structures have been created based on this approach. One of the drawbacks of this approach is that it is not being suitable for wide range of applications, as it may not be possible to represent data as feature vectors.

An alternative direction for research had been similarity search in the more general setting of metric spaces. In this thesis we focus on similarity search methods which assume similarity is defined using a metric distance function. A metric space is defined to be a set of objects S together with a distance function d on pairs of objects that satisfies the following properties $\forall a, b, c \in S$

1. Positivity: $d(a, b) \geq 0, d(a, a) = 0$
2. Symmetry: $d(a, b) = d(b, a)$.
3. Triangle Inequality: $d(a, b) + d(b, c) \geq d(a, c)$.

Positivity property ensure that distance function is defined for pair of objects and distance is not negative. Also it ensures that distance of some object to itself is zero, minimum possible distance, corresponding to intuitive notion object is similar to itself. Symmetry property ensures distance between two object are same regardless of the direction.

Of the distance metric properties, the triangle inequality is the key property for pruning the search space when processing queries. However, in order to make

use of the triangle inequality, we often find ourselves applying the symmetry property. Furthermore, the non-negativity property allows discarding negative values in formulas. The triangle inequality dictates that the distance between two objects is closely related to their distances to a third object. This relation can be seen Figure 2.1. Given distances $d(q, p)$ and $d(p, o)$ upper and lower bounds on $d(q, o)$ can be established.

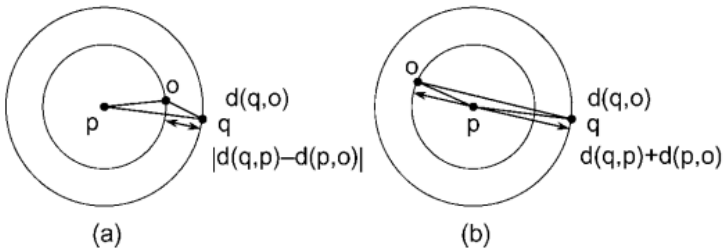

Figure 2.1: Visualization of distance bounds. Given distances $d(q, p)$ and $d(p, o)$ upper and lower bounds on $d(q, o)$ can be established using triangle inequality (a) $d(q, o) \geq |d(q, p) - d(p, o)|$ (b) $d(q, 0) \leq d(q, p) + d(p, o)$

Metric-space indexing structures exploit this fact by appointing a small set of objects to represent the whole population. These objects are called pivots or vantage points. The distances between the pivots and a set of database objects are precomputed and stored in the index structure. At query time, the distance between some of the pivots and the query object is computed. Using the triangle inequality, the distance between a regular database object and the query object can be bounded by their distances to the pivots. If the lower bound of the distance between a database object and the query object is greater than the query radius, it follows that the object is outside the query range, and the object can be eliminated from consideration. In a similar fashion, if the upper bound of the distance is less than the query radius, it follows that the object lies within the range. We call this operation pivoting. Objects that have been classified in this manner are said to be eliminated. Database objects that are not eliminated must have their distances to the query object computed explicitly. The efficiency of an index structure is directly related to the fraction of database objects that can be eliminated through pivoting.

Distance-based indexing methods do not make any assumptions about the

internal structure about objects as long as distance function is defined over all pair of objects in the collection. This level of abstraction enables us the capability of capturing a large variety of similarity search applications. It provides a natural and intuitive way to approach a problem. For example, the distance between two character strings may easily be determined by the edit distance, which is a metric [53]. On the other side, this level of abstraction eliminates some constraints which could be useful in building indexes. For example, vector-based methods can enhance efficiency by processing the dimensions of the vector one at a time. An example of this is incremental distance computation [3], where the distance of the query object to a bounding box is computed one dimension at a time. Another example is the TV-tree [55]. In the TV-tree, new dimensions are introduced only as they are needed.

The advantage of distance-based indexing methods is that once the index has been built, similarity queries can often be performed with a significantly lower number of distance computations than a sequential scan of the entire dataset, as would be the case if no index exists. Another advantage over the multidimensional indexing methods is that different distance metrics can be defined objects and used to index them. Of course, in situations where we may want to apply several different distance metrics, then distance-based indexing techniques have the drawback of requiring that the index be rebuilt for each different distance metric.

There are two main approaches when only distance functions are used in similarity search. First method is to derive artificial features based on inter object distances (e.g., methods described in [22, 42, 57, 89]). In these approaches, goal is to find a mapping F that is defined for all elements of S and query objects which maps original objects to points in k-dimensional space. New distance function d_e defined in k-dimensional space should be as close as possible original distance function d. The advantage of this approach is that it replaces original function d with a new function d_e which is expected to be much less expensive. Another advantage of this approach is that after mapping new points can be indexed using multidimensional indexes. These methods are known as embedding methods and they are also applicable if objects are represented as feature vectors. Advantage

of using embedding methods on features vectors is reduction in the number of dimensions, if the dimensions of newly mapped space k, is smaller than original dimensions of feature vector.

An important constraint on embedding methods is that the mapping F should be contractive [39], which implies that it does not increase the distances between objects. That is, $d_e(F(o_1), F(o_2)) \leq d(o_1, o_2) \forall o_1, o_2 \in S$. This property ensures that there will be no incorrect elimination of objects when processing query using new mapped space and new distance function. Results are later refined using d (e.g., [48, 79]).

Another approach which is used when only distance functions are known is to index objects with respect to their distances from a few selected objects called pivots. Almost all existing index structures for metric similarity search are built around the concept of pivoting. They differ in the way they select pivots, which objects are associated with each pivot, how the pivot distances will be organized and how pivots separate objects. These differences also affect how the querying process will be carried out.

Deciding how pivots partition data is also a differentiating factor among similarity search algorithms. [85] identified two basic partitioning schemes, ball partitioning and generalized hyperplane partitioning.

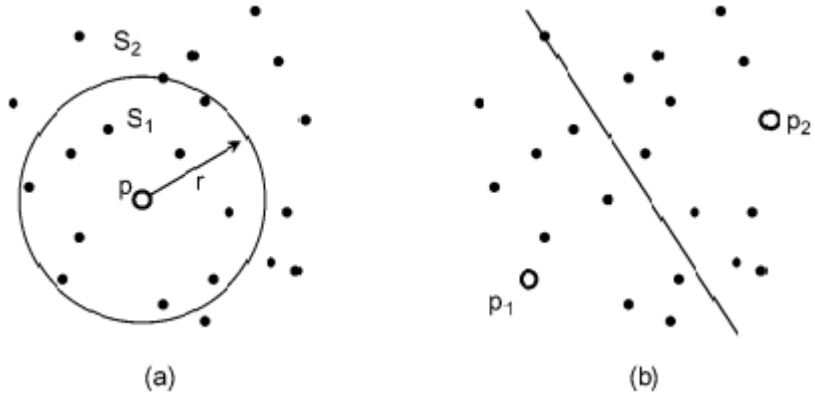

Figure 2.2: Possible partitioning of a set of objects. (a)ball partitioning and (b) generalized hyperplane partitioning.

In ball partitioning, the data set is partitioned based on distances from one

distinguished object, sometimes called a vantage point [93], that is, into the subset that is inside and the subset that is outside a ball around the object (e.g., Figure 2.2(a)).

In generalized hyperplane partitioning, two distinguished objects a and b are chosen and the data set is partitioned based on which of the two distinguished objects is the closest, that is, all the objects in subset A are closer to a than to b, while the objects in subset B are closer to b (e.g., Figure 2.2(b)).

2.2 Survey on Related Work

Some of the earliest distance-based indexing methods are due to [14], but most of the work in this area has taken place in the past decades. Typical of distance based indexing structures are metric trees [85], which are binary trees that result in recursively partitioning a data set into two subsets at each node. The VP-tree [93] stands out as one requiring only a small amount of memory and being able to be constructed efficiently. However it is inferior to others in terms of query performance, including methods like the MVP-tree [9], and GNAT [10], both of which improve performance at the cost of greater space and construction time.

The M-tree [17] and Slim-tree [44] are disk-based structures, and support dynamic manipulations on the index while maintaining the balance of the tree. In order to be able to efficiently handle split and merge operations, however, they keep less precise data than the comparable GNAT structure. This results in poorer query performance.

While most distance based indexing structures are variations on and/or extensions of metric trees, there are also other approaches. Several methods based on distance matrices have been designed [65, 87, 88]. In these methods, all or some of the distances between the objects in the data set are precomputed. Then, when evaluating queries, once we have computed the actual distances of some of the objects from the query object, the distances of the other objects can be estimated based on the precomputed distances. Clearly, these distance matrix methods do

not form a hierarchical partitioning of the data set, but combinations of such methods and metric tree-like structures have been proposed [64]. The SA-tree [66] is another departure from metric trees, inspired by the Voronoi diagram. In essence, the SA-tree records a portion of the Delaunay graph of the data set, a graph whose vertices are the Voronoi cells, with edges between adjacent cells.

Tree structures typically only allow an object to have as many pivots as the height of the tree. This may not be satisfactory for difficult distributions and queries. For this reason tree-based structures are not flexible enough to provide greater elimination power when needed. In contrast, vantage point structures like LAESA [65], Spaghettis [15] and FQA [16] represent another family of solutions. They use more space and construction time, but provide greater efficiency at query time. Although other tree structures also have some parameters that can be adjusted, their improvements are not as pervasive or as dramatic. The shortcomings of vantage points-based methods are the extra computational overhead that they incur, higher construction costs, and higher space usage. If they are allowed to use a sufficient number of pivots, these methods have been shown to outperform other methods in terms of the number of distance computations performed. Some of the structures in this family offer some improvements to the common problems of high space and construction time. The Spaghettis structure reduces computational overhead but uses more space than the common approach. The FQA also reduces overhead, but it uses less precision in the distance information it stores, resulting in reduced performance in terms of the number of distance computations.

Further material on similarity search methods can be found at [66] and [38] which are very good surveys on similarity search.

In the following sections we report similarity search methods under three broad categories: Clustering-based methods, local pivot-based methods, and vantage points-based methods.

2.2.1 Clustering-Based Methods

The basic theme behind clustering-based methods is the use of a hierarchical, tree-based decomposition of the space, where the subtrees are designed to group close objects together. We also observe that each subtree is represented by a single object from the database that is ideally located near the center of the group of objects stored in this subtree.

J. Uhlmann [85] defined the gh-tree, short for generalized hyperplane tree, as one of the first examples in this category. The idea is to pick two objects from the current subset as representatives, and partition the rest of the set into two classes, depending on which representative is closer.

The GNAT tree, presented by S. Brin [10] is a generalization of the gh-tree, where there are more than two representatives. A simple algorithm is given to pick the representatives. According to the algorithm, if we are to select k representatives, we first pick $3 \cdot k$ points randomly. Then, starting with an initial set consisting of one random representative, we incrementally grow the set by adding the point that maximizes the minimum distance to the other representatives.

In addition to its representatives, each node can also maintain the radius of the associated region, that is, the maximum distance of the objects inside a representatives region. This method was used in the M-tree (described below). Another enhancement would be to include the distances between the representatives as well. An even more precise way is used in the GNAT tree. Every representative stores the minimum and maximum distances to the objects in every other subset.

The performance of GNAT, in the best case, has been reported to make more than a factor of 6 fewer distance computations than the VP-tree, while requiring about a factor of 14 more in distance computations in its construction. However, it was reported to be worse than the VP-tree in some cases. The original study [10] also showed that GNAT was outperformed by a variant of the vantage points structure, although no data was given about the parameters used in the construction of this structure. Recent experiments presented by [66], [16] show

indeed that GNAT performs consistently worse than variants of vantage points structures in terms of number of distance computations, while it consumes less space and has less computational overhead.

The M-tree [17] is designed to be a dynamic structure, with emphasis being paid to the structures ability to perform queries efficiently and to optimize I/O performance after a sequence of data insertions. Similar to SS-tree [90], it keeps the distance to the farthest object in a subtree. Maintaining the radius of the representative objects allows it to easily reorganize disk blocks. Splitting a node involves selecting two new representatives and redistributing objects associated with this node among these two new nodes. The M-tree considers all possibilities for a split and chooses the one with tightest covering radius.

The Slim-tree [44] employs a more efficient splitting method. The minimum spanning tree of the objects is generated and the longest arcs of the spanning tree is removed partition the set of objects into two subsets.

2.2.2 Local Pivot-Based Methods

The structures in this category are also tree-based, however, the partitions are based on the distances of objects to either one or two selected objects called pivots. Objects that have similar distances to the pivots are put inside the same subtree, but that does not necessarily mean they are in close proximity of each other. The pivots are only used within their subset, and this is why we call them local pivots. W. Burkhard and R. Keller [14] suggested selecting a random object in the data set and partitioning the rest such that every object having the same distance to the preselected object is placed in the same subset. The tree construction continues recursively on the subset of points at the same distance. Since their application domain produced discrete distance values, it was possible for many points to be at the same distance.

An adaptation of the same basic idea to continuous distance values is the VP-tree, [93]. Such a tree is defined by a branching factor. In order to construct

a vp-tree with a given branching factor k, at a given node, one of the objects is selected as the vantage point, and the distances from the other objects to this vantage point are calculated. Then these objects are partitioned into k groups of roughly equal size based on these distances. In this way a node can have k branches with each subtree having roughly m/k objects, where m denotes the number of objects for that node. The only information that needs to be stored is the vantage point itself, and the $k-1$ distance values, denoted as cutoff[1..k], defining the ranges of distances for each subtree.

A range query of radius r centered at a query point q is answered as follows: at any given node, the distance d between q and the nodes vantage point is calculated. If d is smaller than r, the vantage point is added into the result set. For every subset i of the node defined by the cutoff values, if the interval of the subset, [cutoff [$i-1$], cutoff [i]] intersects the interval $[d-r, d+r]$, then subset i is searched recursively.

A nice feature of the VP-tree is that it is possible to divide the space into many divisions through a single distance calculation. As a result, when doing a search, we need only perform one distance calculation per node. However, as the dimensionality of the data distribution grows, it is well known that for many distributions, the objects tend to cluster around a single distance value [5]. As a result, almost all of the objects are at the same distance to the vantage point. Thus, the distance to the vantage point loses its discriminating power with respect to the objects. Another common way to describe the situation is to visualize the situation in a 3 dimensional space, where the median spheres dividing the branches have very similar radii, subdividing space into thin spherical shells. As a result, objects that are grouped under same subtree tend to be spread around the space rather being close to one another.

The MVP-tree [9] uses two vantage points per node. After partitioning the points with one primary vantage point, the partitions are further divided by using the second vantage point. This way, if we divide the space into m different regions by first vantage point, we will have a total of up to m^2 subsets. It should be noted that the second vantage point uses different cutoff values for each partition

of the first vantage point. This allows the tree to maintain balance by assigning approximately the same number of points to each subset. This occurs at the cost of more space consumption per node. The value of this partitioning approach is that, instead of dividing the space into very thin shells, it strives to produce more tightly clustered subsets, while still achieving the same fanout.

The MVP-tree stores distances to two vantage points at the leaf nodes, making it a hybrid of the vantage-point structures. It is reported to perform up to 80

2.2.3 Vantage-Point Methods

In vantage-point methods the pivots are used to control processing for the entire set of objects instead of having local scope as they do in the previously described methods. A subset of the objects are selected as vantage points. The distance between the pivots and the rest of the objects are computed at initialization time and stored in the database. At query time these precomputed distances are used to eliminate candidates in a way that is similar to local methods. If there are k vantage points, then the basic method performs $k \cdot n$ distance computations at construction and keeps $k \cdot n$ distance values in the index structure. A range query accesses these distance values to determine which objects can be eliminated based on their distances to vantage points. Finally, a pass through all objects not eliminated by use of pivots is performed.

Note that vantage-point methods require extra processing compared to local methods, where determination of the partition at a node is done only for the objects covered by the node. Local methods require storage that is only linear in the database size, whereas vantage-point methods require $O(k \cdot n)$ storage.

A powerful aspect of these methods is that it is possible to use as many pivots as desired at the cost of construction time, which results in higher storage requirements and extra preprocessing time. Nonetheless, this additional effort and space can yield progressively better query performance in terms of the number of distance computations.

The first vantage-point structure that appeared in literature was LAESA [65], as a special case of AESA [87]. There have been some improvements over the basic LAESA algorithm, such as keeping distances to the vantage points sorted and doing binary searches to identify which objects can be eliminated from consideration [67].

The TLAESA structure [64] was proposed as a hybrid method between the LAESA and the gh-tree. The pivots are organized as in a gh-tree, but a distance matrix is also used to provide lower bounds for the distance of the query object to the node representatives. Their experiments were performed in low dimensions, and although were superior to LAESA in terms of total CPU cost, it was inferior in terms of the number of distance computations.

The Spaghettis structure [15] was introduced as a method designed to further decrease computational overhead. Here the distances are sorted in a similar fashion. In addition, every distance has a pointer for the same objects distance in the next array of distances. As done in the case of sorted distances, the feasible ranges are computed for each array using binary search. For each point, its path starting from first array is traced using the pointers. Once the object falls out of range in any of the arrays, we may infer that the object cannot lie within the query region.

The Fixed Queries Array (FQA) [16] is one of the recent global pivot-based methods. It sorts the points according to their distances to the first vantage point, then on the second, and so on. It decreases the precision with which distances are measured, for otherwise the points effectively would be sorted only in their distance to the first pivot. Using this sorted structure, the query algorithm performs binary searches within each distance range. The first pivot is processed as in the sorted-array approach, after that, for each range of objects that has the same discretized distance to the first vantage point, we perform a binary search to find the range that is valid for the second pivot. The search continues in this fashion performing binary searches within ranges.

FQA is unique among vantage-point methods that are designed to reduce computational overhead in that it does not require any additional storage. However

it does not work very well if too many bits are used for the distance values, since this would require that the structure be sorted only by the first pivot. This creates an additional trade-off between the number of bits used for distance storage and extra CPU processing time needed. This comes in addition to the trade-o between number of bits and query performance in terms of distance computations. Their experiments show great improvements in low dimensions, but for 20 dimensional data for a database of one million objects, they estimate FQA would take only 37.6

2.3 KVP Algorithm

In this section KVP structure [18], will be introduced in detail. This structure is unique since it improves both the storage and computational overhead of the classical vantage-points approach. The KVP structure offers a number of benefits:

1. It is a simple data structure and can be implemented relatively easily.
2. It can support dynamic operations like insertion and deletion.
3. It is easily adapted for use as a disk-based structure and its access patterns minimize the number of disk-seek operations.
4. Queries may be executed in parallel.

2.3.1 The KVP Structure

In vantage points all pivots are kept in structure even though not all of them may be useful in query evaluation. In [18], it is reported that it is desirable to use pivots that are particularly close to the query object. Similarly, a pivot to be more effective for objects that are close to or distant from it. This suggest an improvement over keeping all pivots, at index creation time, one can find pivots that are more close or distant to a object, and choose to keep only the distances to these promising pivots.

This is indeed what is done with KVP, the distance relations between the pivots and database elements are computed beforehand at construction time. In addition to reducing CPU overhead by first processing the most promising pivots, one can eliminate distance computations to the less promising pivots, thus decreasing the space requirements. There are two ways this can be implemented. One way would involve the usual layout, where every pivot stores an array of distances to all the database objects. The object distances can be sorted so that binary search can be used to quickly determine set of objects that are eliminated. Another way to implement the basic idea is to have a collection of object entries, where each object entry stores the distances to its selected pivots. The benefit of this latter approach is that it is very easy to insert or delete objects from the database, since there is no global data structure that keeps information about the objects. KVP takes the second approach. Figure 2.3 illustrates the approach.

Other than the fact that KVP only stores a subset of pivot distances, the way it processes queries is identical to the classical global pivot-based method. For each database object it maintains a lower and upper bound for the distance to the query object. Each pivot is used to attempt to tighten these bounds. After processing all possible pivot distances, if the bounds are good enough to either discard the object as out of the query range, or prove that it is within the query range, one avoids computing the actual distance between the object and the query object. Otherwise this distance is computed.

Figure 2.4 shows the query performance of KVP as a function of the number of pivots stored for a query radius of 0.4 in 20 dimensions. The results that are labeled as random choose the next pivot to be used randomly, simulating a classic vantage-points structure. KVP methods first process close and distant vantage points. For example, assume we have a KVP structure that has a pool of 50 prioritized vantage points, which we refer to as KVP 50. In the sorted array of pivot distances 0 through 49, the processing proceeds in the order: 0, 49, 1, 48, 2, and so on. As the number of pivots in the pool is increased, the chances of finding a better suited pivot also increases. Varying the number of pivots provides flexibility to improve query performance by spending more time at construction time without increasing space and CPU overhead.

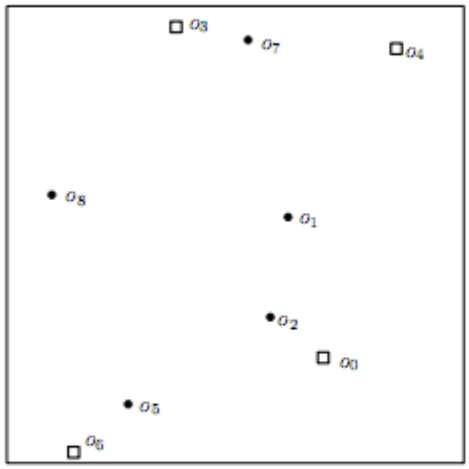

(a)

	o_1	o_2	o_5	o_7	o_8
o_0	0.32	0.16	0.46	0.74	0.73
o_3	0.50	0.68	0.86	0.16	0.45
o_4	0.45	0.67	1.01	0.33	0.83
o_6	0.72	0.54	0.16	1.02	0.60

(b)

obj. id	pivot id	distance	pivot id	distance
1	0	0.32	6	0.72
obj. id	pivot id	distance	pivot id	distance
2	0	0.16	3	0.68
obj. id	pivot id	distance	pivot id	distance
5	6	0.16	4	1.01

(c)

Figure 2.3: A sample database of 9 vectors in 2-dimensional space, and an example of the KVP structure on this database that keeps 2 distance values per database object. (a) The location of objects. Boxes represent objects that have been selected as pivots. (b) The distance matrix between pivots and regular database objects. For each object, the 2 most promising pivot distances are selected to be stored in KVP (indicated by using gray background color). (c) The first three object entries in the KVP. Each object entry keeps the id of the object, and an array of pivot distances.

As seen from the graphs that KVP, can eliminate database objects much faster than the classic approach.

2.3.2 Secondary Storage

Access patterns of pivot-based structures are targeted toward minimizing CPU time, but they are not always suitable to be stored on disk. For example, performing binary search in secondary storage is expensive as it involves many seek

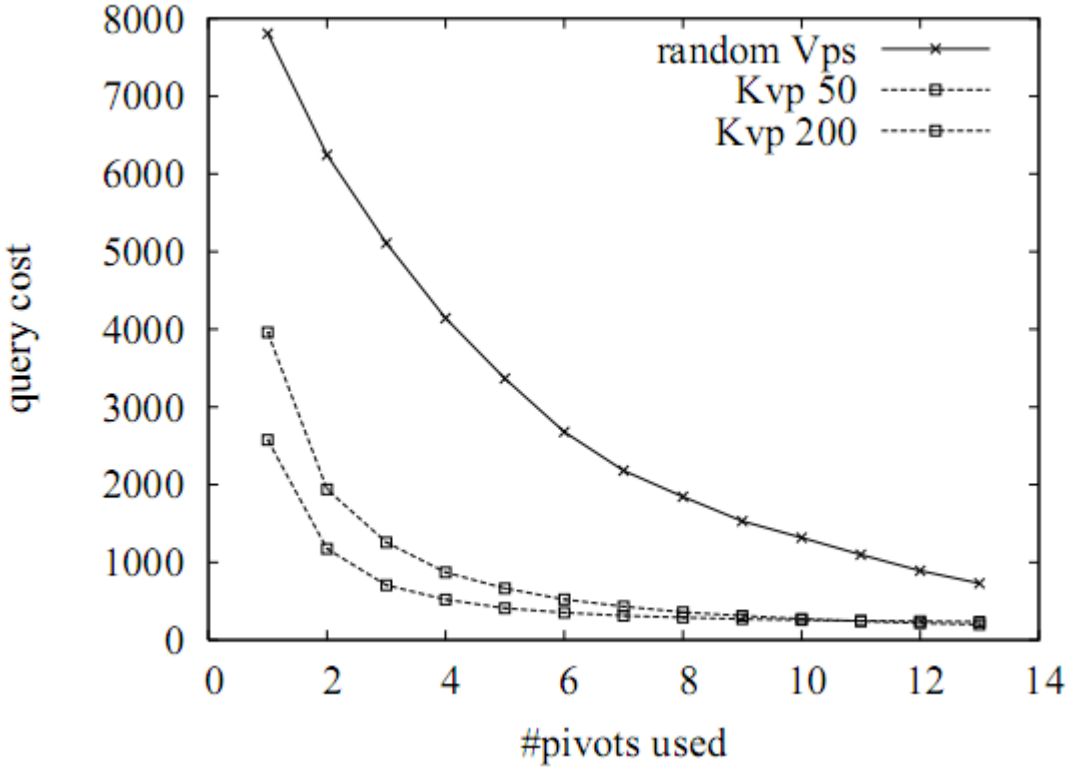

Figure 2.4: Query performance of the KVP structure, for vectors uniformly distributed in 20 dimensions.

operations. Disks are much better at performing sequential scans. The KVP structure is quite amenable for data that are stored on disk. It only requires a sequential scan of distance values. It does not involve a heavy processing burden, so processing time does not dominate over I/O time. It requires relatively little memory, since only the vantage objects, the query object, and the distance vector of the processed object is needed.

2.3.3 Memory Usage

KVP and its variants HKvp and EcKvp store fewer distance values than the classic vantage-point methods [18]. Depending on the parameters of KVP structure, memory usage of KVP changes. KVP structure keeps tracks of indexes used in structure. Also for each object a subset of pivots is selected, and distance from

object to selected pivots is precomputed and stored.

For object collection of n objects, if b_d bits are used for distance values and b_i bits are used for indexes of pivots, and assuming n_{pivot} selected in index construction with $n_{pivotlimit}$ limit per object, memory usage of KVP is m_{KVP},

$$m_{KVP} = n \times (n_{pivotlimit} \times (b_d + b_i)) + n_{pivot} * b_i$$

As with FQA, KVP can decrease memory consumption by discretization, so that fewer bits are used for the distance values. Consider its simplest form where the intervals have equal width, using b bits in a metric space where the maximum distance is D_{max}. This will map distances into buckets of width D_w where

$$D_w = \frac{D_{max}}{2^b}$$

Since all the distances in the same bucket will be assigned the same distance value, the maximum error will be D_w per distance value. Assuming query objects are distributed uniformly, we can approximate the error to$D_w/2$.

Therefore, query process is modified to use $r + \frac{D_{max}}{2}$, instead of r and rest of algorithm stays same. This discretization can improve memory usage considerably, since can be very large n.

2.3.4 Comparison of KVP and Tree-Based Structures

Using a KVP structure, one can easily vary a number of parameters, including the construction cost, the number of pivots used per object, the number of pivots stored per object, the number of pivots processed at query time per object, and the number of bits used per distance value.

In a sense, it is possible to view most of the existing structures as variants of the vantage point-based methods. For example in a VP-tree with a branching factor of k, there is one pivot per node, all the objects in subtrees can be eliminated with their distances to this pivot, and number of branches have an affect similar to the number of bits used. For a database object, there are approximately as

many pivots as the height of the tree. This view explains why changing k in the VP-tree has little affect on query performance, since as k increases and pivots become more precise (which is similar to using more bits), the height of the tree becomes shorter and there are fewer pivots per database object. A major problem with the VP-tree is that the only data that is used are the cutoff values. The individual distances of objects to the pivots are computed but then discarded.

From the perspective of vantage points, it is also easier to see why GNAT with branching factor k improves on the VP-tree. In GNAT, there are k pivots per node, and the distance ranges of k subtree to these pivots are stored. One slight disadvantage of GNAT is that ranges of distances to a pivot can overlap. However, instead of having just one pivot per one, objects in GNAT make use of k pivots.

Tree-based methods have two advantages over the classical vantage points methods. Whereas a pivoting operation involves one object in vantage points, it usually involves groups of objects in tree-based structures. This is something that only cause increase on the CPU overhead, and has a negative impact on the number of distance computations. Secondly, tree-based methods attempt to divide the space into clusters in order to benefit from the locality of pivots. This is similar to what priority vantage points and KVP try to accomplish. While tree structures have varying degrees of success in clustering similar objects together, KVP takes a direct approach and precisely computes the closest pivots. In addition, KVP properly makes use of far pivots as well.

Chapter 3

General Purpose Computing On GPU

Recent developments on graphics chips, known generically as Graphics Processing Units or GPUs, have provided a quite powerful computational units. Researchers and developers have become interested in utilizing this power for general purpose computing, an effort known collectively as GPGPU (for General Purpose computing on the GPU). In this section we summarize the efforts in field of GPGPU, give an overview of the techniques and computational building blocks used to map general purpose computation to graphics hardware, and survey the various general purpose computing tasks to which GPUs have been applied. A quite good survey on this field is provided by Owens et al. [71], which this section is based.

Recent graphics architectures provide tremendous memory bandwidth and computational horsepower. For example, the flagship ATI Radeon HD 5970 ($625 as of January 2010) boasts 256.0 GB/sec memory bandwidth; with 4.64 TeraFLOPS theoretical single precision processing power. Similarly competitor NVIDIA's flagship product GeForce 295 GTX ($475 as of January 2010) has 223.8 GB/sec memory bandwidth. GPUs also use advanced processor technology; for example, the ATI HD 5970 contains 4.3 billion transistors and is built on a 40-nanometer fabrication process.

Graphics hardware is fast and getting faster quickly. In fact graphics hardware performance increasing more rapidly than that of CPUs. The disparity can be attributed to fundamental architectural differences: CPUs are optimized for high performance on sequential code, with many transistors dedicated to extracting instruction-level parallelism with techniques such as branch prediction and out-of-order execution. On the other hand, the highly data-parallel nature of graphics computations enables GPUs to use additional transistors more directly for computation, achieving higher arithmetic intensity with the same transistor count.

Modern graphics architectures have become flexible as well as powerful. Early GPUs were fixed-function pipelines whose output was limited to 8-bit-per-channel color values, whereas modern GPUs now include fully programmable processing units that support vectorized floating point operations on values stored at full IEEE single precision (but note that the arithmetic operations themselves are not yet perfectly IEEE-compliant). High level languages have emerged to support the new programmability of the vertex and pixel pipelines [12, 61, 62]. Additional levels of programmability are emerging with every major generation of GPU (roughly every 18 months). For example, current generation GPUs introduced vertex texture access, full branching support in the vertex pipeline, and limited branching capability in the fragment pipeline. The next generation will expand on these changes and add geometry shaders, or programmable primitive assembly, bringing flexibility to an entirely new stage in the pipeline [6]. The raw speed, increasing precision, and rapidly expanding programmability of GPUs make them an attractive platform for general purpose computation.

Yet the GPU is hardly a computational panacea. Its arithmetic power results from a highly specialized architecture, evolved and tuned over years to extract maximum performance on the highly parallel tasks of traditional computer graphics. The increasing flexibility of GPUs, coupled with some ingenious uses of that flexibility by GPGPU developers, has enabled many applications outside the original narrow tasks for which GPUs were originally designed, but many applications still exist for which GPUs are not (and likely never will be) well suited. Word processing, for example, is a classic example of a pointer chasing application,

dominated by memory communication and difficult to parallelize.

Todays GPUs also lack some fundamental computing constructs, such as efficient scatter memory operations (i.e., indexed write array operations) and integer data operands. The lack of integers and associated operations such as bit-shifts and bitwise logical operations (AND, OR, XOR, NOT) makes GPUs ill-suited for many computationally intense tasks such as cryptography (though upcoming Direct3D 10 class hardware will add integer support and more generalized instructions [6]). Finally, while the recent increase in precision to 32-bit floating point has enabled a host of GPGPU applications, 64-bit double precision arithmetic remains a promise on the horizon. The lack of double precision hampers or prevents GPUs from being applicable to many very large scale computational science problems.

Furthermore, graphics hardware remains difficult to apply to non-graphics tasks. The GPU uses an unusual programming model, so effective GPGPU programming is not simply a matter of learning a new language. Instead, the computation must be recast into graphics terms by a programmer familiar with the design, limitations, and evolution of the underlying hardware. Today, harnessing the power of a GPU for scientific or general purpose computation often requires a concerted effort by experts in both computer graphics and in the particular computational domain. But despite the programming challenges, the potential benefits, a leap forward in computing capability and a growth curve much faster than traditional CPUs are too large to ignore.

3.1 Overview Of Graphics Hardware

In this section we will outline the evolution of the GPU and describe its current hardware and software.

3D graphics applications require high computation rates and exhibit substantial parallelism which differentiate it from more general computation domains. Graphic cards are designed to take advantage of the native parallelism in the

application, allowing higher performance on graphics applications than can be obtained on more traditional microprocessors.

All of today's commodity GPUs structure their graphics computation in a similar organization called the graphics pipeline. This pipeline is designed to allow hardware implementations to maintain high computation rates through parallel execution. The pipeline is divided into several stages. All geometric primitives pass through each stage: vertex operations, primitive assembly, rasterization, fragment operations, and composition into a final image. In hardware, each stage is implemented as a separate piece of hardware on the GPU in what is termed a task parallel machine organization. Figure 3.1 shows the pipeline stages in current GPUs. For more detail on GPU hardware and the graphics pipeline, NVIDIA's GeForce 6 series of GPUs is described by Kilgariff and Fernando [47]. From a software perspective, the OpenGL Programming Guide provides an excellent reference [69].

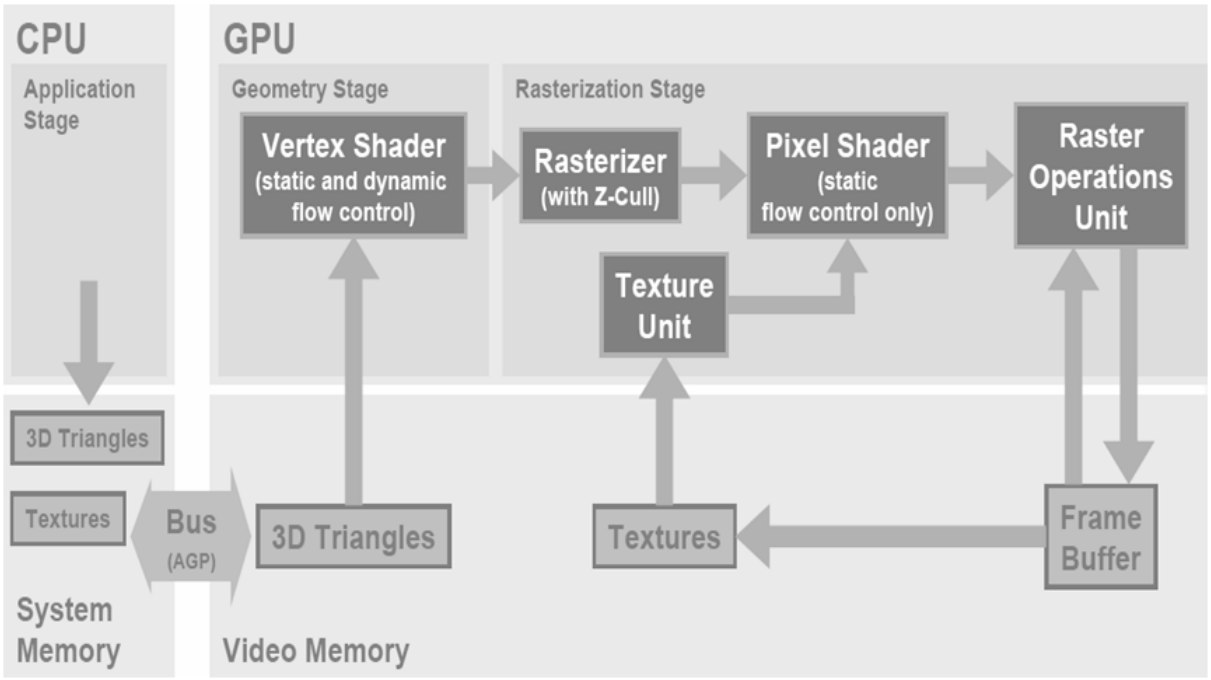

Figure 3.1: The modern graphics hardware pipeline. The vertex and fragment processor stages are both programmable by the user.

3.1.1 Programmable hardware

The graphics pipeline described above was historically a fixed function pipeline, where the limited number of operations available at each stage of the graphics pipeline were hardwired for specific tasks. However, the success of off-line rendering systems such as Pixars RenderMan [86] demonstrated the benefit of more flexible operations, particularly in the areas of lighting and shading. Instead of limiting lighting and shading operations to a few fixed functions, RenderMan evaluated a user defined shader program on each primitive, with impressive visual results.

Over the past seven years, graphics vendors have transformed the fixed function pipeline into a more flexible programmable pipeline. This effort has been primarily concentrated on two stages of the graphics pipeline: the vertex stage and the fragment stage. In the fixed function pipeline, the vertex stage included operations on vertices such as transformations and lighting calculations. In the programmable pipeline, these fixed function operations are replaced with a user defined vertex program. Similarly, the fixed function operations on fragments that determine the fragment's color are replaced with a user defined fragment program.

Each new generation of GPUs has increased the functionality and generality of these two programmable stages. 1999 marked the introduction of the first programmable stage, NVIDIA's register combiner operations that allowed a limited combination of texture and interpolated color values to compute a fragment color. In 2002, ATI's Radeon 9700 led the transition to floating point computation in the fragment pipeline.

The vital step for enabling general purpose computation on GPUs was the introduction of fully programmable hardware and an assembly language for specifying programs to run on each vertex [56] or fragment. This programmable shader hardware is explicitly designed to process multiple data parallel primitives at the same time. In general, these programmable stages input a limited number of 32-bit floating point 4-vectors. The vertex stage outputs a limited number of

32-bit floating point 4-vectors that will be interpolated by the rasterizer; the fragment stage outputs up to 4 floating point 4-vectors, typically colors. Each programmable stage can access constant registers across all primitives and also read-write registers per primitive. The programmable stages have limits on their numbers of inputs, outputs, constants, registers, and instructions; with each new revision of the vertex shader and pixel [fragment] shader standard, these limits have increased.

GPUs typically have multiple vertex and fragment processors. Fragment processors have the ability to fetch data from textures, so they are capable of memory gather. However, the output address of a fragment is always determined before the fragment is processed, and the processor cannot change the output location of a pixel. Vertex processors recently acquired texture capabilities, and they are capable of changing the position of input vertices, which ultimately affects where in the image pixels will be drawn. Thus, vertex processors are capable of both gather and scatter. Unfortunately, vertex scatter can lead to memory and rasterization coherence issues further down the pipeline. Combined with the lower performance of vertex processors, this limits the utility of vertex scatter in current GPUs.

3.2 GPU Programming Model

GPUs are a compelling solution for applications that require high arithmetic rates and data bandwidths. GPUs achieve this high performance through data parallelism, which requires a programming model distinct from the traditional CPU sequential programming model. In this section, we briefly introduce the GPU programming model using both graphics API terminology and the terminology of the more abstract stream programming model, because both are common in the literature.

The stream programming model exposes the parallelism and communication

patterns inherent in the application by structuring data into streams and expressing computation as arithmetic kernels that operate on streams. Owens [70] discuss the stream programming model in the context of graphics hardware, and the Brook programming system [12] offers a stream programming system for GPUs.

Because typical scenes have more fragments than vertices, in modern GPUs the programmable stage with the highest arithmetic rates is the fragment stage. A typical GPGPU program uses the fragment processor as the computation engine in the GPU. Such a program is structured as follows [32]:

1. First, the programmer determines the data parallel portions of his application. The application must be segmented into independent parallel sections. Each of these sections can be considered a kernel and is implemented as a fragment program. The input and output of each kernel program is one or more data arrays, which are stored (sometimes only transiently) in textures in GPU memory. In stream processing terms, the data in the textures comprise streams, and a kernel is invoked in parallel on each stream element.

2. To invoke a kernel, the range of the computation (or the size of the output stream) must be specified. The programmer does this by passing vertices to the GPU. A typical GPGPU invocation is a quadrilateral (quad) oriented parallel to the image plane, sized to cover a rectangular region of pixels matching the desired size of the output array. Note that GPUs excel at processing data in two dimensional arrays, but are limited when processing one dimensional arrays.

3. The rasterizer generates a fragment for every pixel location in the quad, producing thousands to millions of fragments.

4. Each of the generated fragments is then processed by the active kernel fragment program. Note that every fragment is processed by the same fragment program. The fragment program can read from arbitrary global memory locations (with texture reads) but can only write to memory locations corresponding to the location of the fragment in the frame buffer (as determined

by the rasterizer). The domain of the computation is specified for each input texture (stream) by specifying texture coordinates at each of the input vertices, which are then interpolated at each generated fragment. Texture coordinates can be specified independently for each input texture, and can also be computed on the fly in the fragment program, allowing arbitrary memory addressing.

5. The output of the fragment program is a value (or vector of values) per fragment. This output may be the final result of the application, or it may be stored as a texture and then used in additional computations. Complex applications may require several or even dozens of passes (multipass) through the pipeline.

While the complexity of a single pass through the pipeline may be limited (for example, by the number of instructions, by the number of outputs allowed per pass, or by the limited control complexity allowed in a single pass), using multiple passes allows the implementation of programs of arbitrary complexity.

3.2.1 GPU Program Flow

Flow control is a fundamental concept in computation. Branching and looping are such basic concepts that it can be daunting to write software for a platform that supports them to only a limited extent. The latest GPUs support vertex and fragment program branching in multiple forms, but their highly parallel nature requires care in how they are used. This section surveys some of the limitations of branching on current GPUs and describes a variety of techniques for iteration and decision making in GPGPU programs. Harris and Buck [33] provide more detail on GPU flow control.

3.2.1.1 Hardware mechanisms for flow control

There are three basic implementations of data parallel branching in use on current GPUs: predication, MIMD branching, and SIMD branching.

Architectures that support only predication do not have true data dependent branch instructions. Instead, the GPU evaluates both sides of the branch and then discards one of the results based on the value of the Boolean branch condition. The disadvantage of predication is that evaluating both sides of the branch can be costly, but not all current GPUs have true data dependent branching support. The compiler for high level shading languages like Cg or the OpenGL Shading Language automatically generates predicated assembly language instructions if the target GPU supports only predication for flow control.

In Multiple Instruction Multiple Data (MIMD) architectures that support branching, different processors can follow different paths through the program. In Single Instruction Multiple Data (SIMD) architectures, all active processors must execute the same instructions at the same time. The only MIMD processors in a current GPU are the vertex processors of the NVIDIA GeForce 6 and 7 series and NV40 and G70 based Quadro GPUs. Classifying GPU fragment processors is more difficult. The programming model is effectively Single Program Multiple Data (SPMD), meaning that threads (pixels) can take different branches. However, in terms of architecture and performance, fragment processors on current GPUs process pixels in SIMD groups. Within a SIMD group, when evaluation of the branch condition is identical for all pixels in the group, only the taken side of the branch must be evaluated. However, if one or more of the processors evaluates the branch condition differently, then both sides must be evaluated and the results predicated. As a result, divergence in the branching of simultaneously processed fragments can lead to reduced performance.

3.2.1.2 Moving branching up the pipeline

Because explicit branching can hamper performance on GPUs, it is useful to have multiple techniques to reduce the cost of branching. A useful strategy is to move flow control decisions up the pipeline to an earlier stage where they can be more efficiently evaluated.

Static Branch Resolution On the GPU, as on the CPU, avoiding branching inside inner loops is beneficial. For example, when evaluating a partial differential equation (PDE) on a discrete spatial grid, an efficient implementation divides the processing into multiple loops: one over the interior of the grid, excluding boundary cells, and one or more over the boundary edges. This static branch resolution results in loops that contain efficient code without branches. (In stream processing terminology, this technique is typically referred to as the division of a stream into substreams.) On the GPU, the computation is divided into two fragment programs: one for interior cells and one for boundary cells. The interior program is applied to the fragments of a quad drawn over all but the outer one pixel edge of the output buffer. The boundary program is applied to fragments of lines drawn over the edge pixels. Static branch resolution is further discussed by Goodnight et al. [25].

Z-Cull Precomputed branch results can be taken a step further by using another GPU feature to entirely skip unnecessary work. Modern GPUs have a number of features designed to avoid shading pixels that will not be seen. One of these is Z-cull. Z-cull is a hierarchical technique for comparing the depth (Z) of an incoming block of fragments with the depth of the corresponding block of fragments in the Z-buffer. If the incoming fragments will all fail the depth test, then they are discarded before their pixel colors are calculated in the fragment processor. Thus, only fragments that pass the depth test are processed, work is saved, and the application runs faster. In fluid simulation, land locked obstacle cells can be masked with a z-value of zero so that all fluid simulation computations will be skipped for those cells. If the obstacles are fairly large, then a lot of work is saved by not processing these cells. Harris and Buck provide pseudo code [33] for the technique.

Data Dependent Looping With Occlusion Queries Another GPU feature designed to avoid drawing what is not visible is the hardware occlusion query (OQ). This feature provides the ability to query the number of pixels updated by a rendering call. These queries are pipelined, which means that they provide a way to get a limited amount of data (an integer count) back from the GPU without stalling the pipeline (which would occur when actual pixels are read back). Because GPGPU applications almost always draw quads with known pixel coverage, OQ can be used with fragment kill functionality to get a count of fragments updated and killed. This allows the implementation of global decisions controlled by the CPU based on GPU processing. Harris and Buck provide pseudo code for the technique [33].

3.2.2 GPU Programming Systems

In this section we look at the high level languages that have been developed for GPU programming, and the debugging tools that are available for GPU programmers. Code profiling and tuning tends to be a very architecture specific task. GPU architectures have evolved very rapidly, making profiling and tuning primarily the domain of the GPU manufacturer. As such, we will not discuss code profiling tools in this section.

3.2.2.1 High Level Shading Languages

Most high level GPU programming languages today share one thing in common: they are designed around the idea that GPUs generate pictures. As such, the high level programming languages are often referred to as shading languages. That is, they are a high level language that compiles a shader program into a vertex shader and a fragment shader to produce the image described by the program.

Cg [61], HLSL, and the OpenGL Shading Language all abstract the capabilities of the underlying GPU and allow the programmer to write GPU programs in a more familiar C-like programming language. They do not stray far from

their origins as languages designed to shade polygons. All retain graphics specific constructs: vertices, fragments, textures, etc. Cg and HLSL provide abstractions that are very close to the hardware, with instruction sets that expand as the underlying hardware capabilities expand. The OpenGL Shading Language was designed looking a bit further out, with many language features (e.g. integers) that do not directly map to hardware available today.

Sh is a shading language implemented on top of C++ [62]. Sh provides a shader algebra for manipulating and defining procedurally parameterized shaders. Sh manages buffers and textures, and handles shader partitioning into multiple passes. Sh also provides a stream programming abstraction suitable for GPGPU programming.

3.2.3 GPGPU languages and libraries

More often than not, the graphics centric nature of shading languages makes GPGPU programming more difficult than it needs to be. As a simple example, initiating a GPGPU computation usually involves drawing a primitive. Looking up data from memory is done by issuing a texture fetch. The GPGPU program may conceptually have nothing to do with drawing geometric primitives and fetching textures, yet the shading languages described in the previous section force the GPGPU application writer to think in terms of geometric primitives, fragments, and textures. Instead, GPGPU algorithms are often best described as memory and math operations, concepts much more familiar to CPU programmers. The programming systems below attempt to provide GPGPU functionality while hiding the GPU specific details from the programmer.

The Brook programming language extends ANSI C with concepts from stream programming [12]. Brook can use the GPU as a compilation target. Brook streams are conceptually similar to arrays, except all elements can be operated on in parallel. Kernels are the functions that operate on streams. Brook automatically maps kernels and streams into fragment programs and texture memory.

Accelerator is a system from Microsoft Research that aims to simplify GPGPU programming by providing a high level data parallel programming model in a library that is accessible from within traditional imperative programming languages [82]. Accelerator translates data parallel operations on the fly to GPU pixel shaders, demonstrating significant speedups over C versions running on the CPU.

CGiS is a data parallel programming language from the Saarland University Compiler Design Lab with similar aims to Brook and Accelerator, but with a slightly different approach [63]. Like Brook, CGiS provides stream data types, but instead of explicit kernels that run on the GPU, the language invokes GPU computation via a built in data parallel forall operator.

The Glift template library provides a generic template library designed to simplify GPU data structure design and separate GPU algorithms from data structures [51]. Glift defines GPU computation as parallel iteration over the elements of a data structure. The model generalizes the stream computation model and connects GPGPU with CPU based parallel data structure libraries such as the Standard Template Adaptive Parallel Library (STAPL). The library integrates with a C++, Cg, and OpenGL GPU development environment.

CUDA (an acronym for Compute Unified Device Architecture) is a parallel computing architecture developed by NVIDIA. CUDA is the computing engine in NVIDIA graphics processing units or GPUs that is accessible to software developers through industry standard programming languages. Programmers use 'C for CUDA' (C with NVIDIA extensions), compiled through a PathScale Open64 C compiler, to code algorithms for execution on the GPU. CUDA architecture supports a range of computational interfaces including OpenCL and DirectCompute. Third party wrappers are also available for Python, Fortran, Java and Matlab.

AMD first released its Stream Computing SDK (v1.0), in December 2007 under the AMD EULA, to be run on Windows XP. The SDK includes "Brook+", an AMD hardware optimized version of the Brook language developed by Stanford University, itself a variant of the ANSI C (C language), open-sourced and optimized for stream computing. The AMD Core Math Library (ACML) and

AMD Performance Library (APL) also be included as a part of SDK. Another important part of the SDK, the Compute Abstraction Layer (CAL), is a software development layer aimed for low-level access, through the CTM hardware interface, to the GPU architecture for performance tuning software written in various high-level programming languages.

Finally, the OpenCL (Open Computing Language) is a framework for writing programs that execute across heterogeneous platforms consisting of CPUs, GPUs, and other processors. OpenCL includes a language (based on C99) for writing kernels (functions that execute on OpenCL devices), plus APIs that are used to define and then control the platforms. OpenCL provides parallel computing using task-based and data-based parallelism.

OpenCL is analogous to the open industry standards OpenGL and OpenAL, for 3D graphics and computer audio, respectively. OpenCL extends the power of the GPU beyond graphics (GPGPU). OpenCL is managed by the non-profit technology consortium Khronos Group (http://www.khronos.org/opencl/).

3.2.4 Debugging tools

Support for debugging on GPUs is fairly limited, when compared with CPU. The advent of GPGPU programming makes it clear that a GPU debugger should have similar capabilities as traditional CPU debuggers, including variable watches, program break points, and single-step execution. GPU programs often involve user interaction. While a debugger does not need to run the application at full speed, the application being debugged should maintain some degree of interactivity. A GPU debugger should be easy to add to and remove from an existing application, should mangle GPU state as little as possible, and should execute the debug code on the GPU, not in a software rasterizer. Finally, a GPU debugger should support the major GPU programming APIs and vendor-specific extensions.

There are a few different systems for debugging GPU programs available to use, but nearly all are missing one or more of the important features that are

present in cpu debuggers.

gDEBugger [2] and GLIntercept [83] are tools designed to help debug OpenGL programs. Both are able to capture and log OpenGL state from a program. gDEBugger allows a programmer to set breakpoints and watch OpenGL state variables at runtime, as well as to profile applications using GPU hardware performance signals. There is currently no specific support for debugging shaders, but both support runtime shader editing.

The Microsoft Shader Debugger [1], however, does provide runtime variable watches and breakpoints for shaders. The shader debugger is integrated into the Visual Studio IDE, and provides all the same functionality programmers are used to for traditional programming. Unfortunately, debugging requires the shaders to be run in software emulation rather than on the hardware. In contrast, the Apple OpenGL Shader Builder also has a sophisticated IDE and actually runs shaders in real time on the hardware during shader debug and edit. The downside to this tool is that it was designed for writing shaders, not for computation. The shaders are not run in the context of the application, but in a separate environment designed to help facilitate shader writing.

While many of the tools mentioned so far provide a lot of useful features for debugging, none provide any support for shader data visualization or printf-style debugging. Sometimes this is the single most useful tool for debugging programs. The Image Debugger [4] was among the first tools to provide this functionality by providing a printf-like function over a region of memory. The region of memory gets mapped to a display window, allowing a programmer to visualize any block of memory as an image. The Image Debugger does not provide any special support for shader programs, so programmers must write shaders such that the output gets mapped to an output buffer for visualization.

The Shadesmith Fragment Program Debugger [74] was the first system to automate printf-style debugging while providing basic shader debugging functionality like breakpoints, program stepping, and programmable scale and bias for the image printf. While Shadesmith represents a big step in the right direction for GPGPU debugging, it still has many limitations, the largest of which is that

Shadesmith is currently limited to debugging assembly language shaders. Additionally, Shadesmith only works for OpenGL fragment programs, and provides no support for debugging OpenGL state.

3.3 GPGPU Techniques

In this section we describe some of the building blocks of GPU computation.

3.3.1 Stream operations

There are several fundamental operations on streams that many GPGPU applications implement. These operations are: map, reduce, scatter and gather, scan, stream filtering, sort, and search. In the following sections we define each of these operations.

3.3.1.1 Map

Given a stream of data elements and a function, map will apply the function to every element in the stream. The GPU implementation of map is straightforward, and perhaps best illustrated with an example. Assume we have a stream of data with values. We would like to compute squares of these values. A kernel to do this would multiply each element in the stream by itself to produce the output stream. This application of a function to an input stream is the essence of the map operation.

3.3.1.2 Reduce

Sometimes a computation requires computing a smaller stream from a larger input stream, possibly to a single element stream. This type of computation is

called a reduction. For example, a reduction can be used to compute the sum or maximum of all the elements in a stream.

On GPUs, reductions can be performed by alternately rendering to and reading from a pair of textures. On each rendering pass, the size of the output, the computational range, is reduced by one half. In general, we can compute a reduction over a set of n data elements in $O(\frac{n}{p}logn)$ time steps using the parallel GPU hardware (with p elements processed in one time step), compared to O(n) time steps for a sequential reduction on the CPU. To produce each element of the output, a fragment program reads two values, one from a corresponding location on either half of the previous pass result buffer, and combines them using the reduction operator (for example, addition or maximum). These passes continue until the output is a one-by-one buffer, at which point we have our reduced result. For a two dimensional reduction, the fragment program reads four elements from four quadrants of the input texture, and the output size is halved in both dimensions at each step. Buck et al. describe GPU reductions in more detail in the context of the Brook programming language [12].

3.3.1.3 Scatter and Gather

Two fundamental memory operations with which most programmers are familiar are write and read. If the write and read operations access memory indirectly, they are called scatter and gather respectively. A scatter operation looks like the C code d[a] = v where the value v is being stored into the data array d at address a. A gather operation is just the opposite of the scatter operation. The C code for gather looks like v = d[a].

The GPU implementation of gather is essentially a dependent texture fetch operation. A texture fetch from texture d with computed texture coordinates a performs the indirect memory read that defines gather. Unfortunately, scatter is not as straightforward to implement. Fragments have an implicit destination address associated with them: their location in frame buffer memory. A scatter operation would require that a program change the framebuffer write location of

a given fragment, or would require a dependent texture write operation. Since neither of these mechanisms exist on today's GPU, GPGPU programmers must resort to various tricks to achieve a scatter. These tricks include rewriting the problem in terms of gather; tagging data with final addresses during a traditional rendering pass and then sorting the data by address to achieve an effective scatter; and using the vertex processor to scatter (since vertex processing is inherently a scattering operation). Buck has described these mechanisms for changing scatter to gather in greater detail [11].

3.3.1.4 Scan

A simple and common parallel algorithmic building block is the all-prefix-sums operation, also known as scan [37]. For each element in a sequence of elements, prefix-sum computes the sum of all previous elements in the sequence. The first implementation of scan on GPUs was presented by Horn and demonstrated for the applications of collision detection and subdivision surfaces [41]. Hensley et al. used a similar scan implementation to generate summed-area tables on the GPU [36]. The algorithms of Horn and Hensley et al. were efficient in the number of passes (O(log n)) executed, but required O(n log n) total work, a factor of log n worse than the optimal sequential work complexity of O(n). Greß et al. presented O(n) algorithms for GPUs [30]. Greß et al. construct a list of potentially intersecting bounding box pairs and utilize scan to remove the non-intersecting pairs. The algorithm of Sengupta et al. is notable for its method of switching from a tree-based work-efficient algorithm to Horns brute-force algorithm as it approaches the root of the tree. This hybrid approach more efficiently uses all of the parallelism provided by the GPU.

3.3.1.5 Stream filtering

Many algorithms require the ability to select a subset of elements from a stream, and discard the rest. The location and number of elements to be filtered is variable and not known a priori. Example algorithms that benefit from this stream

filtering operation include simple data partitioning (where the algorithm only needs to operate on stream elements with positive keys and is free to discard negative keys) and collision detection (where only objects with intersecting bounding boxes need further computation).

Horn has described a technique called stream compaction [41] that implements stream filtering on the GPU. Using a combination of scan and search, stream filtering can be achieved in O(log n) passes.

3.3.1.6 Sort

A sort operation allows us to transform an unordered set of data into an ordered set of data. Sorting is a classic algorithmic problem that has been solved by several different techniques on the CPU. Many of these algorithms are data-dependent and generally require scatter operations; therefore, they are not directly applicable to a clean GPU implementation. Data-dependent operations are difficult to implement efficiently, and scatter is not implemented for fragment processors on today's GPUs. To make efficient use of GPU resources, a GPU-based sort should be oblivious to the input data, and should not require scatter.

Most GPU-based sorting implementations [31, 46, 76, 75] have been based on sorting networks. The main idea behind a sorting network is that a given network configuration will sort input data in a fixed number of steps, regardless of the input data. Additionally, all the nodes in the network have a fixed communication pattern. The fixed communication pattern means the problem can be stated in terms of gather rather than scatter, and the fixed number of stages for a given input size means the sort can be implemented without data-dependent branching. This yields an efficient GPU-based sort, with an overall $O(nlog^2n)$ computational complexity.

Sorting networks can also be implemented efficiently using the texture mapping and blending functionalities of the GPU [29]. In each step of the sorting network, a comparator mapping is created at each pixel on the screen and the

color of the pixel is compared against exactly one other pixel. The comparison operations are implemented using the blending functionality and the comparator mapping is implemented using the texture mapping hardware, thus entirely eliminating the need for fragment programs. Govindaraju et al. have also analyzed the cache efficiency of sorting network algorithms and presented an improved bitonic sorting network algorithm with a better data access pattern and data layout. The precision of the underlying sorting algorithm using comparisons with fixed-function blending hardware is limited to the precision of the blending hardware. For example, the current blending hardware has 16-bit floating point precision. Alternatively, the limitation to 16-bit values on current GPUs can be alleviated by using a single-line fragment program for evaluating the conditionals, but the fragment program implementation on current GPUs is slightly slower than the fixed-function pipeline.

Greß and Zachmann [31] present a novel algorithm, GPU-ABiSort, to further enhance the sorting performance on GPUs. Their algorithm is based on an adaptive bitonic sorting algorithm and achieves an optimal performance of O(n log n) for any computation time T in the range of $O(log^2 n) \leq T \leq O(nlogn)$. The algorithm maps well to the GPU and is able to achieve good performance on an NVIDIA 7800 GTX GPU.

GPUs have also been used to efficiently perform 1-D and 3-D adaptive sorting of sequences [27]. Unlike sorting network algorithms, the computational complexity of adaptive sorting algorithms is dependent on the extent of disorder in the input sequence, and work well for nearly-sorted sequences. The extent of disorder is computed using Knuths measure of disorder. Given an input sequence I, the measure of disorder is defined as the minimal number of elements that need to be removed for the rest of the sequence to remain sorted. The algorithm proceeds in multiple iterations. In each iteration, the unsorted sequence is scanned twice. In the first pass, the sequence is scanned from the last element to the first, and an increasing sequence of elements M is constructed by comparing each element with the current minimum. In the second pass, the sorted elements in the increasing sequence are computed by comparing each element in M against the current minimum in I M. The overall algorithm is simple and requires only

comparisons against the minimum of a set of values. The algorithm is, therefore, useful for fast 3D visibility ordering of elements where the minimum comparisons are implemented using the depth buffer [27].

External memory sorting algorithms are used to organize large terabyte-scale datasets. These algorithms proceed in two phases and use limited main memory to order the data. Govindaraju et al. [26] present a novel external memory sorting algorithm to sort billion-record wide-key databases using a GPU. In the first phase, GPUTeraSort pipelines the following tasks on the CPU, disk controller and GPU: read disk asynchronously, build keys, sort using a GPU, generate runs and write disk. In this phase, GPUTeraSort uses the data parallelism and high memory bandwidth on GPUs to quickly sort large runs. In the second phase, GPUTera-Sort uses a similar task pipeline to read, merge and write the runs. GPUTeraSort offloads the compute-intensive and memory intensive tasks to the GPU; therefore, it is able to achieve higher I/O performance and better memory performance than CPU-only algorithms.

3.3.1.7 Search

The last stream operation we discuss, search, allows us to find a particular element within a stream. Search can also be used to find the set of nearest neighbors to a specified element. Nearest neighbor search is used extensively when computing database queries (e.g. find the 10 nearest restaurants to point X). When searching, we will use the parallelism of the GPU not to decrease the latency of a single search, but rather to increase search throughput by executing multiple searches in parallel.

Binary Search The simplest form of search is the binary search. This is a basic algorithm, where an element is located in a sorted list in O(log n) time. Binary search works by comparing the center element of a list with the element being searched for. Depending on the result of the comparison, the search then recursively examines the left or right half of the list until the element is found, or is determined not to exist.

The GPU implementation of binary search [41, 76, 75] is a straightforward mapping of the standard CPU algorithm to the GPU. Binary search is inherently serial, so we can not parallelize lookup of a single element. That means only a single pixel's worth of work is done for a binary search. We can easily perform multiple binary searches on the same data in parallel by sending more fragments through the search program.

Nearest Neighbor Search Nearest neighbor search is a slightly more complicated form of search. In this search, we want to find the k nearest neighbors to a given element. During a nearest neighbor search, candidate elements are maintained in a priority queue, ordered by distance from the seed element. At the end of the search, the queue contains the nearest neighbors to the seed element.

Unfortunately, the GPU implementation of nearest neighbor search is not as straightforward. We can search a k-d tree data structure [23], but it is difficult to efficiently maintain a priority queue. The important detail about the priority queue is that candidate neighbors can be removed from the queue if closer neighbors are found. Purcell et al. propose a data structure for finding nearest neighbors called the kNN-grid [76, 75]. The grid approximates a nearest-neighbor search, but is unable to reject candidate neighbors once they are added to the list. The quality of the search then depends on the density of the grid and the order in which candidate neighbors are visited during the search.

3.3.2 Data Structures

Every GPGPU algorithm must operate on data stored in an appropriate structure. This section describes the data structures used thus far for GPU computation. Effective GPGPU data structures must support fast and coherent parallel accesses as well as efficient parallel iteration, and must also work within the constraints of the GPU memory model.

GPU data are almost always stored in texture memory. To maintain parallelism, operations on these textures are limited to read-only or write-only access

within a kernel. Write access is further limited by the lack of scatter support. Outside of kernels, users may allocate or delete textures, copy data between the CPU and GPU, copy data between GPU textures, or bind textures for kernel access. Lastly, most GPGPU data structures are built using 2D textures for three reasons. First, GPU's 2D memory layout and rasterization pattern (i.e., iteration traversal pattern) are closely coupled to deliver the best possible memory access pattern. Second, the maximum 1D texture size is often too small for most problems, and third, current GPUs cannot efficiently write to a slice of a 3D texture.

Iteration In modern C/C++ programming, algorithms are defined in terms of iteration over the elements of a data structure. The stream programming model performs an implicit data parallel iteration over a stream. Iteration over a dense set of elements is usually accomplished by drawing a single large quad. This is the computation model supported by Brook, Sh, and Scout. Complex structures, however, such as sparse arrays, adaptive arrays, and grid-of-list structures often require more complex iteration constructs [8, 49, 50]. These range iterators are usually defined using numerous smaller quads, lines, or point sprites.

Generalized Arrays via Address Translation The majority of data structures used thus far in GPGPU programming are random-access multidimensional containers, including dense arrays, sparse arrays, and adaptive arrays. Lefohn et al. [51] show that these virtualized grid structures share a common design pattern. Each structure defines a virtual grid domain (the problem space), a physical grid domain (usually a 2D texture), and an address translator between the two domains. A simple example is a 1D array represented with a 2D texture. In this case, the virtual domain is 1D, the physical domain is 2D, and the address translator converts between them.

In order to provide programmers with the abstraction of iterating over elements in the virtual domain, GPGPU data structures must support both virtual-to-physical and physical-to-virtual address translation. For example, in the 1D array example above, an algorithm reads from the 1D array using a virtual-to-physical (1D-to-2D) translation. An algorithm that writes to the array, however,

must convert the 2D pixel (physical) position of each stream element to a 1D virtual address before performing computations on 1D addresses. A number of authors describe optimization techniques for pre-computing these address translation operations before the fragment processor [8, 49, 50]. These optimizations pre-compute the address translation using the CPU, the vertex processor, and/or the rasterizer.

The Brook programming systems provide virtualized interfaces to most GPU memory operations for contiguous, multi-dimensional arrays. Sh provides a subset of the operations for large 1D arrays. The Glift template library provides virtualized interfaces to GPU memory operations for any structure that can be defined using the programmable address translation paradigm. These systems also define iteration constructs over their respective data structures [12, 51, 62].

3.4 GPGPU applications

In this section we survey a range of applications and tasks implemented on graphics hardware.

The use of computer graphics hardware for general purpose computation has been an area of active research for many years, beginning on machines like the Ikonas [19], and the Pixel Machine [73]. Pixars Chap [54] was one of the earliest processors to explore a programmable SIMD computational organization, on 16-bit integer data; Flap, described three years later, extended Chaps integer capabilities with SIMD floating point pipelines. These early graphics computers were typically graphics compute servers rather than desktop workstations. Early work on procedural texturing and shading was performed on the UNC Pixel-Planes 5 and PixelFlow machines [68]. This work can be seen as precursor to the high level shading languages in common use today for both graphics and GPGPU applications. The PixelFlow SIMD graphics computer was also used to crack UNIX password encryption [45].

The wide deployment of GPUs in the last several years has resulted in an

increase in experimental research with graphics hardware. The earliest work on desktop graphics processors used non-programmable (fixed-function) GPUs. Lengyel et al. used rasterization hardware for robot motion planning [52]. Bohn used fixed-function graphics hardware in the computation of artificial neural networks [7]. Convolution and wavelet transforms with the fixed-function pipeline were realized by Hopf [40].

Programmability in GPUs first appeared in the form of vertex programs combined with a limited form of fragment programmability via extensive user-configurable texture addressing and blending operations. While these dont constitute a true ISA, so to speak, they were abstracted in a very simple shading language in Microsoft's pixel shader version 1.0 in Direct3D 8.0. Trendall and Stewart gave a detailed summary of the types of computation available on these GPUs [84]. A major limitation of this generation of GPUs was the lack of floating point precision in the fragment processors. Strzodka showed how to combine multiple 8-bit texture channels to create virtual 16-bit precise operations [80], and Harris analyzed the accumulated error in boiling simulation operations caused by the low precision [34].

Below we briefly explain some GPU applications classified under some major application areas:

Physically based simulation Early GPU-based physics simulations used cellular techniques such as cellular automata (CA). Greg James of NVIDIA demonstrated the Game of Life cellular automata and a 2D physically based wave simulation running on NVIDIA GeForce 3 GPUs. Harris et al. used a Coupled Map Lattice (CML) to simulate dynamic phenomena that can be described by partial differential equations, such as boiling, convection, and chemical reaction-diffusion [35].

Several groups have used the GPU to successfully simulate fluid dynamics. Several papers presented solutions of the Navier-Stokes equations (NSE) for incompressible fluid flow on the GPU [8, 25, 49].

Other recent work includes flow calculations around arbitrary obstacles [8,

49].

Rigid body simulation for computer games has been shown to perform very well on GPUs. Havok FX demonstrated an API for rigid body and particle simulation on GPUs, featuring full collisions between rigid bodies and particles, as well as support for simulating and rendering on separate GPUs in a multi-GPU system. Running on a PC with dual NVIDIA GeForce 7900 GTX GPUs and a dual-core AMD Athlon 64 X2 CPU, Havok FX achieves more than a 10x speedup running on GPUs compared to an equivalent, highly optimized multithreaded CPU implementation running on the dual-core CPU alone.

Signal and image processing The high computational rates of the GPU have made graphics hardware an attractive target for demanding applications such as those in signal and image processing.

Motivated by the high arithmetic capabilities of modern GPUs, several projects have developed GPU implementations of the fast Fourier transform (FFT) [12, 43]. (The GPU Gems 2 chapter by Sumanaweera and Liu, in particular, gives a detailed description of the FFT and their GPU implementation.) In general, these implementations operate on 1D or 2D input data, use a Cooley-Tukey radix-2 decimation-in-time approach (with the exception of Jansen et al.s decimation-in-frequency approach [43]), and require one fragment program pass per FFT stage.

Yang and Pollefeys used GPUs for real-time stereo depth extraction from multiple images [92]. Their pipeline first rectifies the images using per-pixel projective texture mapping, then computes disparity values between the two images, and, using adaptive aggregation windows and cross checking, chooses the most accurate disparity value. Their implementation was more than four times faster than a comparable CPU-based commercial system.

Woetzel and Koch addressed a similar problem using a plane sweep algorithm. The approach of Woetzel and Koch begins with a plane sweep over images from multiple cameras and pays particular attention to depth discontinuities [91].

Strzodka and Garbe describe a real-time system that computes and visualizes motion on 640480 25 Hz 2D image sequences using graphics hardware [81]. Their system assumes that image brightness only changes due to motion (due to the brightness change constraint equation). Using this assumption, they estimate the motion vectors from calculating the eigenvalues and eigenvectors of the matrix constructed from the averaged partial space and time derivatives of image brightness.

Erra introduced fractal image compression to the GPU with a brute-force Cg implementation that achieved a speedup of over 100:1 over a comparable CPU implementation [20].

Image/Video Processing Frameworks Apple's Core Image and Core Video frameworks allow GPU acceleration of image and video processing tasks; the open-source framework Jahshaka uses GPUs to accelerate video compositing.

Graphics Perhaps not surprisingly, one of the early areas of GPGPU research was aimed at improving the visual quality of GPU-generated images. Many of the techniques described below accomplish this by simulating an entirely different image generation process from within a fragment program (e.g. a ray tracer). These techniques use the GPU strictly as a computing engine. Other techniques leverage the GPU to perform most of the rendering work, and augment the resulting image with global effects.

Ray tracing is a rendering technique based on simulating light interactions with surfaces. It is nearly the reverse of the traditional GPU rendering algorithm: the color of each pixel in an image is computed by tracing rays out from the scene camera and discovering which surfaces are intersected by those rays and how light interacts with those surfaces. The ray-surface intersection serves as a core for many global illumination algorithms. The earliest GPGPU ray tracing systems demonstrated that the GPU was capable of not only performing ray-triangle intersections, but that the entire ray tracing computation including acceleration structure traversal and shading could be implemented entirely within a set of fragment programs [75].

Nearly all of the major ray tracing acceleration structures have been implemented in some form on the GPU: uniform grids [75], k-d trees [23]. All of these structures are limited to accelerating ray tracing of static scenes. The efficient implementation of dynamic ray tracing acceleration structures is an active research topic for both CPU and GPU based ray tracers.

Some of the early GPU based ray tracing work required special drivers, as features like fragment programs and floating point buffers were relatively new and rapidly evolving. There are currently open-source GPU-based ray tracers that run with standard drivers and APIs.

Geometric computing GPUs have been widely used for performing a number of geometric computations. These geometric computations are used in many applications including motion planning, virtual reality, etc. and include the following.

Collision Detection GPU-based collision detection algorithms rasterize the objects and perform either 2D or 2.5-D overlap tests in screen space. Furthermore, visibility computations can be performed using occlusion queries and used to compute both intra and inter object collisions among multiple objects [60].

Transparency Computation Transparency computations require the sorting of 3D primitives or their image space fragments in a back-to-front or a front-to-back order and can be performed by image-space occlusion queries [27].

Particle Tracing Particle tracingand in general generation of vector-field visualizing primitives has been an active field of research, particularly since the availability of geometry creation and modification features on GPUs. Recent applications make use of either the copy-to-vertex-buffer, the render-to-vertex-buffer [46] or the vertex-texture-fetch functionality to displace primitives.

The performance of many geometric algorithms on GPUs is also dependent upon the layout of polygonal meshes; a better layout more effectively utilizes the vertex caches on GPUs. Yoon et al. proposed a novel method for computing cache-oblivious layouts of polygonal meshes and applied it to

improve the performance of geometric applications such as view-dependent rendering and collision detection on GPUs [94]. Their method does not require any knowledge of cache parameters and does not make assumptions on the data access patterns of applications. A user constructs a graph representing an access pattern of an application, and the cache-oblivious algorithm constructs a mesh layout that works well with the cache parameters. The cache-oblivious algorithm was able to achieve 220 times improvement on many complex scenarios without any modification to the underlying application or the runtime algorithm.

Databases and data mining Database Management Systems (DBMSs) and data mining algorithms are an integral part of a wide variety of commercial applications such as online stock market trading and intrusion detection systems. Many of these applications analyze large volumes of online data and are highly computation-and memory-intensive. As a result, researchers have been actively seeking new techniques and architectures to improve the query execution time. The high memory bandwidth and the parallel processing capabilities of the GPU can significantly accelerate the performance of many essential database queries such as conjunctive selections, aggregations, semi-linear queries and join queries. Govindaraju et al. compared the performance of SQL queries on an NVIDIA GeForce 6800 against a 2.8 GHz Intel Xeon processor. Preliminary comparisons indicate up to an order of magnitude improvement for the GPU over a SIMD-optimized CPU implementation [28].

GPUs are highly optimized for performing rendering operations on geometric primitives and can use these capabilities to accelerate spatial database operations. Recent research has also focused attention on the effective utilization of graphics processors for fast stream mining algorithms. In these algorithms, data is collected continuously and the underlying algorithm performs continuous queries on the data stream as opposed to one-time queries in traditional systems. Many researchers have advocated the use of GPUs as stream processors for compute-intensive algorithms [12]. Recently, Govindaraju et al. have presented fast streaming algorithms using the blending

and texture mapping functionalities of GPUs [29]. Data is streamed to and from the GPU in real time, and a speedup of 25 times is demonstrated on online frequency and quantile estimation queries over high end CPU implementations. The high growth rate of GPUs, combined with their substantial processing power, are making the GPU a viable architecture for commercial database and data mining applications.

Chapter 4

Implementation of Algorithms

Implementation work in this thesis is performed in C++ language and both CPU and GPU executable versions of the implementations are provided. Since several algorithms with different implementations are to be compared, a library to support development is also implemented. Currently it contains implementations of Brute Force Scan and KVP algorithm for CPU and GPU execution. Library provides a framework to expand and integrate new algorithms as well as utilities for different GPGPU programing environments. Tools to evaluate performance for each index are also provided.

The library architecture closely mimics the goals and structure of similarity search. The goal of similarity searching is, given a finite set of objects U, and a distance function d(x, y) defined among objects of U, preprocess U and build a data structure so that similarity searches can be carried out on that set. Although several other queries like approximate search, joins are also possible the library focuses on the two most popular types of queries:

1. Range queries: given a query object $q \in U$, and a radius r, retrieve all database objects within distance r to q)

2. k-nearest-neighbor queries: given a query object $q \in U$ and an integer K, retrieve the K database objects closest to q, breaking ties arbitrarily).

There are three main interfaces in the library: MetricSpaceObject, MetricSpace, and Index. These interfaces provide a basis to implement new metric space and indexes easily. During design goal was to interpret these interfaces as black boxes, on which the only operations one can perform are specified in the interface, and nothing else should be assumed on them. Since we assume these objects are black-boxes another interface GPUStreamSerializable is also introduced. Although this interface has nothing to with similarity search it provides a mechanism to transfer these object to GPU memory, if it is required. This approach also enables seamless integration of GPU versions of the algorithms.

First of these interfaces MetricSpaceObject interface is the highest level description of metric space objects and provides essentially a (usually opaque) data type. It provides basic operations like copying a metric object from an existing object. It also extends GPUSerializable interface, so that object can be transferred to GPU memory, if algorithm is to be run on GPU.

Interface GPUSerializable provides and abstraction on how to load metric spaces objects or index structures to GPU memory. Basically this interface defines functionality to serialize a structure in a memory location. GPU programming model requires each parameters to kernels to be either be streams or basic types like int, float etc. Therefore by defining this interface a generic mechanism to load each index or metric space to GPU is provided. Functions specified by this interface are as follows:

virtual void* allocateBuffer(int objectCount): allocates a buffer big enough to contain objectCount objects to be used in GPU transfer.

virtual void freeBuffer(void *ptr): frees a previously allocated buffer for GPU transfer

virtual int getStreamSize(int objectCount): returns the size of serialized structure for objectCount object in bytes.

virtual void* toStream(void* streamBuffer,int offset,int size): converts size objects starting from index offset to memory location pointed by streamBuffer. If streamBuffer is null necessary memory is allocated first.

Interface MetricSpace describes collections of metric space object plus a distance function among pairs of such objects. It also implements functions to load/save objects from/to disk, etc. Metric spaces can be either randomly generated (e.g. uniformly distributed unitary cubes) or gathered from some public repository. In addition to extending GPUStreamSerializable interface, it defines following functions:

virtual int size(): returns number of objects existing in collection.

virtual char* getPath(): returns path to the object collection file.

virtual void setPath(const char* path): sets path to file where object collection is to be saved/found.

virtual int open(): opens and initializes metric space.

virtual bool isOpen(): returns true if metric space is opened before, false otherwise

virtual void close(): closes and frees resources used by metric space.

virtual MetricSpaceObject* getObject(int index): return object specified by the index.

virtual MetricSpaceObject* createNewObject(): creates a new metric space object and returns a pointer to it.

virtual float distance(MetricSpaceObject *o1, MetricSpaceObject *o2): computes distance between two given metric space objects

virtual bool generateRandomObjects(int argc,char argv):** generates a random object collection

virtual bool convertToBinary(const char* path,const char*name): converts text databases two binary versions

Currently only vector metric spaces are implemented by library. Class VectorSpace implements generation, persistence and loading of metric vector spaces.

Index Interface provides an abstraction for data structures for indexing metric spaces, and should work with any of them. An index implements functions to build the index from a database, run range and kNN queries, etc. This interface also extends GPUSerializable interface, for index to run on GPU. Complete list of functions defined in this interface are as follows:

virtual char* getName(): returns unique name for the index implementation.

virtual char* getPath(): returns path to the index file.

virtual void setPath(const char* path): sets path to file where index is to be saved/found.

virtual MetricSpace* getMetricSpace(): returns the metric space implementation that index uses

virtual void setMetricSpace(MetricSpace* space): sets the metric space implementation that index uses

virtual Index* GPUImplementation(): returns GPU implementation of the index

virtual Index* CPUImplementation(): returns CPU implementation of the index

virtual void build (int n, int argc, char **argv): builds index using given parameters. argc specifies number of arguments, argv contains the arguments

virtual void save(): saves index

virtual void load(): load index

virtual RadiusQueryResults* search (MetricSpaceObject* qobj, float r, RadiusQueryResults* results): performs range query

virtual KNNQueryResults * searchNN (MetricSpaceObject* qobj, int k, KNNQueryResults * results): performs k-nearest neighbor query

virtual void getSearchTaskConstraints(SearchTaskConstraints *constraints): returns any constraints that index imposes on search tasks

virtual SearchTask* createTask(int taskID,int offset,int size): creates a search task for size number of objects with given taskID for objects starting at index offset

virtual void initialize(SearchTask* task): initializes index, before queries are made.

virtual RadiusQueryResults* search (SearchTask* task, MetricSpaceObject* qobj, float r,RadiusQueryResults* results): performs range query as specified in search task

virtual KNNQueryResults * searchNN (SearchTask* task, MetricSpaceObject* qobj, int k,KNNQueryResults * results): performs k-nearest neighbor query as specified in search task

Notice in this interface two different versions of range and k-nearest neighbor query search functions are specified. The first specifications performs queries on whole set of objects contained in metric space. Second versions performs queries only on some objects specified by search tasks. Search task are abstraction on decomposing search. Base interface only defines a task id for the task, number of objects to be processed and index of object from which search will start. This allows parallelization of similarity searches, without requiring index implementation to address the issue. Some other dispatcher class assigns this tasks to available GPUs or CPU cores present in the system.

Library currently supports two queries, range and k-nearest neighbor. Classes RadiusQueryResults and KNNQueryResults provides necessary structures to easily manage result set.

Queries are performed by calling corresponding search function of index. Specific implementations for range and k-nearest neighbor provides functionality to handle generation of a query object, loading and persistence of queries.

In this design, to add a new index or metric space, it suffices to provide only concrete implementation for corresponding object implementing necessary interfaces.

4.1 Brute Force Search Implementation on GPU

Brute Force Search is implemented to provide a benchmark for KVP algorithm as well as to observe performance gains to be obtained by utilizing GPU.

Brute Force Search of distances involves computing distance of each object in object collection with query object. Computed distances compared against query radius and a result set of objects whose distance to query object is less than or equal query object is returned.

The first step of GPU adaptation of the algorithm is to load object collection into graphic card texture memory. ATI Cal and Brook+ requires this collection to be converted into kernel streams first. Although specific function calls differ, both frameworks basically requires objects to be serialized as bytes to some memory location first. Thus objects are serialized into float array of appropriate size, Figure 4.1 shows how this serialization is performed.

Brook+ and ATI Cal framework requires objects to be serialized into some system memory before they can be copied into GPU local memory. Thus a naive implementation requires double data copying, luckily by suitable implementation of metric vector spaces, this double copy requirement is bypassed. Metric space object structure designed so as match GPU memory representation, and just pointer to this structure is passed to memory copy functions.

Another optimization worth of noting was to use float4 as stream type, this optimization allowed us benefit from graphic card architecture as it enabled execution of four multiplications concurrently in one instruction, which will be explained while discussing distance computations kernel.

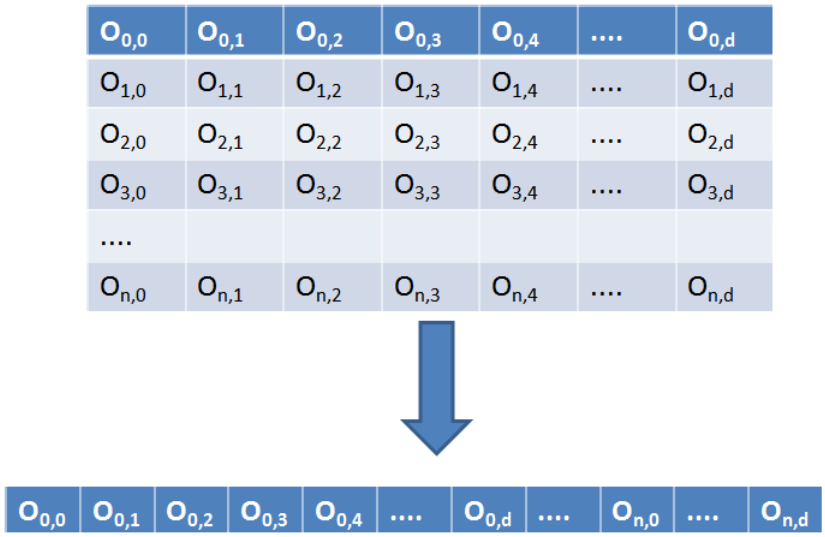

Figure 4.1: Serialized representation of objects.

ATI Graphics cards used in implementation has limits on stream sizes. ATI Radeon HD 4870x2 only supports 8192 elements per 1D stream, and for ATI Radeon HD 5870 this limit is 16384. Thus you can not allocate streams whose element number greater than this specified limits. For 2D streams this limit is 8192x8192 and 16384x16384 respectively. Brook+ framework provide automatic conversion of 1D arrays to 2D arrays whose size exceeds the limit. ATI CAL framework does not provide automatic conversion of 1D arrays to 2D arrays, so in order to overcome this limitations, all streams that are to be expected to have more than 8192 are allocated as 2D streams. This limit on streams requires a address translation code, and extra computation steps in GPU implementation.

Once objects are loaded into GPU, only query and radius information changes per query. This information is also serialized as objects and transferred to GPU and GPU kernel is called from the CPU side.

3 Kernel functions are used to implement brute force linear scan on GPU. The first kernel is used for Brook+ implementation to compute distance of an object to query object which given in listing 4.1

```
1  kernel float distL2D(float4 object[],int offset,
2                       float4 queryObject[],int d)
3  {
4    int i = 0;
5    float4 diff;
6    float4 total = float4 (0.0f,0.0f,0.0f,0.0f);
7
8    for (i=0;i<d;i++){
9      diff = object[offset+i]-queryObject[i];
10     total += diff*diff;
11   }
12   return sqrt(total.x+total.y+total.w+total.z);
13 }
```

Listing 4.1: Brook+ Kernel for distance computation

This kernel is a reduce kernel which computes distance from query object to a given object using euclidean distance. First parameter is a float4 stream representing objects. Second parameter named offset, and represents the starting index of object whose distance to query object is to be computed. Third parameter is query object stream and finally fourth parameter is the dimension of the object divided by four.

distL2D kernel computes euclidean distance of query object to some given object. Lines 4-5 initializes variables used in kernel. Local variable i used as loop counter, diff to hold difference between each vector coordinate, total is used to hold running cumulative sum of squared differences. Local variables are defined as float4, which is basically a record of 4 floats. Advantage of this type is that it enables use of packed arithmetic operations. Packed version of arithmetic operations performs the operation simultaneously on the corresponding fields of the record. Consider following code:

```
float val1x,val2x,rx;
float val1y,val2y,ry;
float val1w,val2w,rw;
float val1z,val2z,rz;

rx = val1x*val2x;
ry = val1y*val2y;
rw = val1w*val2w;
rz = val1z*val2z;
```

which is equivalent to following code

```
float4 val1,val2,r;

r = val1*val2;
```

because of packed operation instructions available in GPU.

In each loop iteration difference between vector coordinates is computed, squared and added to running sum total. As it can be seen loop does not run number of dimension times, as would expected. It runs number of dimensions/4 times because of and architecture of GPU supports 4 operations in one instruction. As depicted in figure 4.2, by using float4 type loop is optimized by performing 4 coordinate pair differences in one instruction.

Similarly running sum and squaring of difference in line 10, also benefits by performing operations in one instruction. Instead of d * (1 subtraction+1 multiplication+1 addition), packed versions of operations are performed in GPU thus number of required clock cycles is reduced by 4. Finally in line 12 each separate running sum in float4 structure is summed and square root of total is returned as distance.

Second kernel used in Brook+ implementation is given in listing 4.2

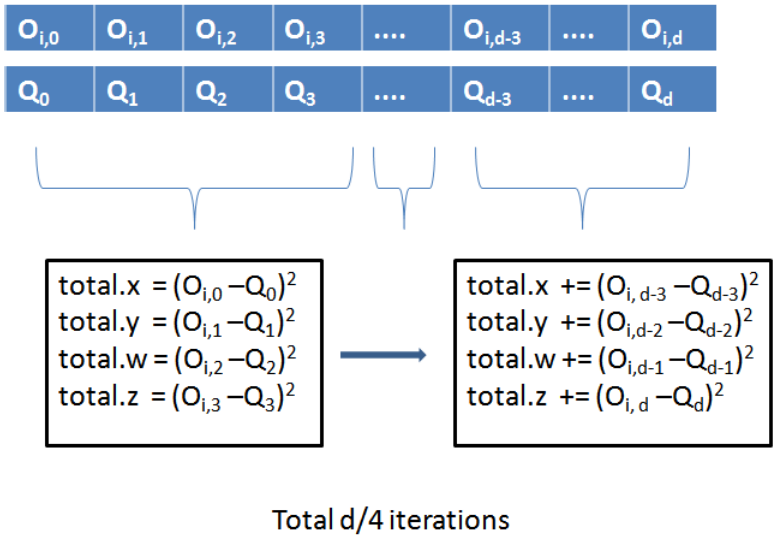

Figure 4.2: Packed instruction execution.

```
1 kernel void BROOK_linear_scan_r_query(float4 object[], int d, float4
      queryObject[],
2   out float distance<>)
3 {
4   distance = distL2D(object, instance().x*d, queryObject, d);
5 }
```

Listing 4.2: Brook+ Kernel for Brute Force Search

This kernel calls first kernel for each object in objects collection. Although no for loop is present, code defined in the kernel is invoked per each output stream element, which is named distance. First parameter of kernel is object stream which holds objects whose distance is to be computed. Second parameter is dimensions of objects /4 and third parameter is query object stream. In line 4 kernel invokes distL2D kernel by passing object and query streams, along with dimension information. Index of object whose distance to query object is to be computed is determined by instance() primitive of Brook+ language, which returns index of output stream for which kernel is invoked.

ATI Cal implementation of Brute Force Search kernel is given in listing 4.3

```
1  kernel void CAL_linear_scan_r_query(int indexMetaData[],
2    float4 object[][], float4 queryObject[], out float distance<>)
3  {
4    int i=0;
5    int width = indexMetaData[0];
6    int d = indexMetaData[2];
7    float4 diff;
8    float4 total = float4 (0.0f,0.0f,0.0f,0.0f);
9    int2 idx = instance().xy;
10   int actualIndex = (idx.y*width+idx.x);
11
12   if (actualIndex >= indexMetaData[1]){
13     return;
14   }
15   actualIndex = actualIndex * d;
16
17   idx.x = actualIndex % width;
18   idx.y = actualIndex / width;
19
20
21   for (i=0;i<d;i++){
22     diff = object[idx.y][idx.x]-queryObject[i];
23     total += diff*diff;
24     idx.x++;
25     if (idx.x >= width ){
26       idx.y ++;
27       idx.x = 0;
28     }
29   }
30   distance = sqrt(total.x+total.y+total.w+total.z);
31 }
```

Listing 4.3: ATI CAL Kernel for Brute Force Search

This kernel differs from Brook+ kernel as there is no automatic address translation support in ATI Cal framework, also distance computation kernel is unfolded. First parameter of this kernel is indexMetaData, which consists of several values guiding computation in kernel. First value in indexMetaData stream is

supposed to be the width of distance stream, hence object stream. Second value is the number of objects in object collection and third value is the number of dimensions/4.

Lines 4 to 10 consists of initialization of local variables used in kernel.

In line 12 a check is performed to terminate kernel if computations is not necessary. This is because of the stream size limits imposed by graphic card. Since we can not allocate arbitrary sized 1D streams, 2D stream is allocated if limit is surpassed. Width of 2D stream is set to maximum allowed value and height is computed accordingly. This approach can sometimes allocate unnecessary space, if total number of objects is not multiple of maximum 2D stream width. Line 12 checks this condition and exits from kernel without any further computation.

Line 17 and 18 translates 1D index to 2D stream index and in for loop starting on line 21 computes euclidean distance of object to query object in similar fashion as in Brook+ kernel.

4.2 KVP Implementation GPU

KVP algorithm is chosen for implementation because it readily supports parallelization.This structure is unique since it improves both the storage and computational overhead of the classical vantage-points approach. The KVP structure offers a number of benefits:

1. It is a simple data structure and can be implemented relatively easily.
2. It can support dynamic operations like insertion and deletion.
3. It is easily adapted for use as a disk-based structure and its access patterns minimize the number of disk-seek operations.
4. Queries may be executed in parallel.

KVP algorithm utilizes precomputed object to pivot distances to reduce number of distance computations in a similarity search. Given a query, algorithm first computes distances to pivots from query object. These distances, along with precomputed object to pivot distances are used to set a bound on query to object distances. If distance bounds are found to be greater than search radius query object is discarded. If upper bound for distance is smaller than radius, then object is added to result set without any need for actual distance computation.

The first step of GPU adaptation of the algorithm is to load object collection into graphic card texture memory as in brute force search method. This step is performed similar to GPU adaptation of Brute Force search.

Second step is to load index structure into memory. The same limitations on streams sizes and memory copy requirements apply, so KVP representation is modified to adapt GPU. Original implementation of KVP stores a record per object which consist of object pivot distances and indexes to pivots whose distances is precomputed. In our implementation, they are represented as a single array of object to pivots distances and pivot indexes respectively. This representation enables loading of KVP structure into graphic card memory without temporary memory copy operations.

Another modification to original implementation was to change data structure which hold the indexes of pivots used in KVP. Since GPU adaptation of KVP designed to utilize all graphic processing units available on a system, this representation posed a problem. When there is more than one graphic processor present in the system processing of query is divided between each graphic processing unit by assigning a part of object collection to each graphic processing unit. Thus not every object is present in each graphical processing unit, and indexes to pivots are not useful. So instead of passing indexes of pivots in collection, pivot object is passed instead.

Once objects are loaded into GPU, only query and radius information changes per query. This information is also serialized as objects and transferred to GPU and GPU kernel is called from the CPU side.

5 Kernel functions are used to implement brute KVP algorithm on GPU. The first kernel is used for address translation of indexes for objects. As noted before this was due to stream size limitations of graphics cards. Kernel listed in listing 4.4 takes two arguments, actual index of object in 1D streams and maximum 2D width allowed by graphic card. Using this values objects index is calculated and result is returned in structure consisting of two integers.

```
1 kernel int2 translateAddress(int actualIndex,int width)
2 {
3   int2 idx;
4   idx.x = actualIndex % width;
5   idx.y = actualIndex / width;
6   return idx;
7 }
```

Listing 4.4: ATI CAL kernel for Address Translation

Next kernel is implemented to perform distance computations between query object and a object whose index is given. Listing for this kernel is show in listing 4.5.

```
1  kernel float distL2D(float4 object[][],int d,float4 queryObject[],
       int logicalIndex,int width)
2  {
3    int i=0;
4    float4 diff;
5    float4 total = float4 (0.0f,0.0f,0.0f,0.0f);
6
7    int2 idx = translateAddress(logicalIndex*d,width);
8
9    for (i=0;i<d;i++){
10     diff = object[idx.y][idx.x]-queryObject[i];
11     total += diff*diff;
12     idx.x++;
13     if (idx.x >= width ){
14       idx.y ++;
15       idx.x = 0;
16     }
17   }
18   return sqrt(total.x+total.y+total.w+total.z);
19 }
```

Listing 4.5: ATI CAL kernel for Object distance computation

distL2D kernel after local variable initialization, actual index of object whose distance is to be computed is found. Then euclidean distance computation is performed similar to Brute Force Search.

The kernel presented on listing 4.6 used for computing distance from query object to each pivot in KVP structure. It consists of one line, a call to distL2D kernel with appropriate parameters. After execution of this kernel queryPivot-Distance stream contains distance of query to each pivot, which is later used on computation of object to query distance bounds.

```
1 kernel void computeQueryToPivotDistances(int indexMetaData[], float4
      object[][], float4 queryObject[], out float queryPivotDistance<>)
2 {
3   queryPivotDistance = distL2D(object, indexMetaData[2], queryObject,
        instance().x, indexMetaData[0]);
4 }
```

Listing 4.6: ATI CAL kernel for Query object to pivot distance computation

Kernel computeDistanceBounds which is show in listing 4.7, computes distance bounds for an object whose index is specified. First argument of kernel, indexMetaData stream, is used to pass index and graphic card specific information to kernel. First value of stream contains maximum 2D width supported by graphic card. Second value is the number of objects in object collection. Third value is dimensions of objects divided by four, as objects are represented as float4 streams. Lastly fourth value is the number of pivots selected during KVP index construction. Next parameter of the kernel is a stream used to represent object pivot distances. Third parameter is a stream representing indexes of pivots whose distance to objects is precomputed. Fourth parameter is the query to pivot distances. Last two parameters are query radius and index of the object whose distance bounds is to be computed.

After initialization in computeDistanceBounds kernel, for loop in line 10 computes minimum and maximum possible distance of object to query object using precomputed object to pivot distance. In each iteration of loop, a pivot next in sequence of pivots is selected (Line 11). According triangle inequality of metric spaces, upper bound for this objects distance should be d(query,pivot)+d(pivot,object). If this maximum possible distance is greater than query radius, which implies that object is query result set, this maximum distance value is returned without considering other pivots. If it is not smaller or equal to query radius than minimum possible distance is computed. Again this minimum on distance value is checked against query radius. If minimum possible distance value is greater than query radius, which implies that object is not definitely in query result set, minimum distance is returned without considering remaining

pivots. If no conclusive bounds on object distance is can not be established, next pivot is used to establish the distance bound.

```
1  kernel float computeDistanceBounds(int indexMetaData[],float
       nodePivotDistance[][],int nodePivotIndex[][],float
       queryPivotDistance[],float r,int logicalIndex)
2  {
3    int numberOfNodePivots = indexMetaData[3];
4    int2 idx = translateAddress(logicalIndex*numberOfNodePivots,
         indexMetaData[0]);
5    int i = 0;
6    float minDist = 0.0f;
7    float maxDist = 0.0f;
8    int pivotIndex = 0;
9
10   for (i=0;i<numberOfNodePivots;i++){
11     pivotIndex = nodePivotIndex[idx.y][idx.x];
12     maxDist = queryPivotDistance[pivotIndex] + nodePivotDistance[idx
           .y][idx.x];
13     if (maxDist <= r )
14       return maxDist;
15
16         minDist = abs(queryPivotDistance[pivotIndex] -
               nodePivotDistance[idx.y][idx.x]);
17         if (minDist > r )
18       return minDist;
19
20     idx.x++;
21     if (idx.x >= indexMetaData[0] ){
22       idx.y ++;
23       idx.x = 0;
24     }
25   }
26   return -1.0f;
27 }
```

Listing 4.7: ATI CAL kernel for object distance bound computation

After examining all possible pivots for query to object distance bounds, if no usable distance bound can be established, i.e. objects presence of elimination

from query result set can be proved, object is marked for distance computation by returning special value -1.

Last kernel implementation for KVP algorithm is presented in listing 4.8. This kernel starts computation by checking whether this invocation is for a valid object. If it is not it immediately returns. If it is for a valid object, first distance bounds on object is computed. If result of distance bound computation is conclusive so as to decide whether include object in result set or eliminate it kernel returns. If not distance from query to object is computed (Line 11).

```
1  kernel void computeObjectQueryDistances(int indexMetaData[], float4
       object[][], float nodePivotDistance[][], int nodePivotIndex[][],
       float queryPivotDistance[], float r, float4 queryObject[], out float
        distance<>)
2  {
3    int4 index = instance();
4    int objectIndex = index.y*indexMetaData[0]+index.x;
5    float dist;
6
7    if (objectIndex >= indexMetaData[1])
8      return;
9    dist = computeDistanceBounds(indexMetaData, nodePivotDistance,
         nodePivotIndex, queryPivotDistance, r, objectIndex);
10   if (dist == -1.0f)
11     dist = distL2D(object, indexMetaData[2], queryObject, objectIndex,
           indexMetaData[0]);
12   distance = dist;
13 }
```

Listing 4.8: ATI CAL kernel for KVP algorithm

4.3 Filtering Results on GPU

Adaptations of search algorithms presented in this thesis rely on the fragment processor, which operates across a large set of output memory locations, consuming a fixed number of input elements per location and operating a small program

on those elements to produce a single output element in that location. Because the fragment program must write its results to a preordained memory location, it is not able to vary the amount of data that it outputs according to the input data it processes.

Many algorithms are difficult to implement under these limitations, specifically, algorithms that reduce many data elements to few data elements. The reduction of data by a fixed factor has been carefully studied on GPUs [12]; such operations require an amount of time linear in the size of the data to be reduced. However, nonuniform reductionsthat is, reductions that filter out data based on its content on a per element basis have been less thoroughly studied, yet they are required for a number of interesting applications.

Search algorithms presented in this thesis does not specifically require distance filtering to be performed on GPU. Filtering of results, i.e. deciding whether an object is in result set based on its distance which is basically a condition check on an array of distance values, can be performed in CPU side. Even filtering result set on CPU provides speed up of several times in execution times, as bulk of the time is spent on distance computations. Thus and implementation provided still benefit acceleration by utilization of graphic cards, yet if this filtering can be performed efficiently in GPU, additional speed up can be obtained by eliminating some data transfer from GPU to CPU. In order to explore this possibility a result set filtering algorithm that makes it possible to perform filtering GPU is presented is also designed.

Our problem is to eliminate objects from result set that have distance value greater than specified query radius. Several approaches can be used. The most obvious method for compaction can be a stable sort to eliminate the records; however, using bitonic sort to do this will result in a running time of O(n (log n)2) ([13]). Instead, we present a technique here that uses a scan ([37]) to obtain a running count of the number of distances that are smaller or equal to query radius, and then use a scatter pass to compact them, for a final running time of O(n log n) similar the algorithm given [72] .

Given a list of objects, to decide where a particular object redirect itself, it

is sufficient to count the number of distances that are smaller or equal to query radius to the left of the each distance, then move the object that many records to the left. On a parallel system, the cost of finding a running count is actually O(n log n). The multipass technique to perform a running sum is called a scan. It starts by counting the number of valid distance in the current record. This number is saved to a stream for further processing. The kernel for this part is listed in listing 4.9

```
1  kernel void initialize_results_index(float distance<>,float radius ,
       out int results_index<>,out int results_index2<>)
2  {
3    if (distance > radius) {
4      results_index = 0;
5      results_index2 = 0;
6    }
7    else {
8      results_index = 1;
9      results_index2 = 1;
10   }
11 }
```

Listing 4.9: ATI CAL Kernel for Result Set Filtering Initialization

Now each record in the stream holds the number of valid distances (distances thats are smaller or equal to query radius) at its location, which is 0 or 1. This can be used to the algorithm's advantage in another pass, where the stream sums itself with records indexed to the left and saves the result to a new stream. Now each record in the new stream effectively has added the number of valid distances at its current position and left of it. The subsequent steps add their values to values indexed at records of increasing powers of two to their left, until the power of two exceeds the length of the input array. This process is illustrated in Figure 4.3.

Kernel used for this multipass operation is presented in listing 4.10

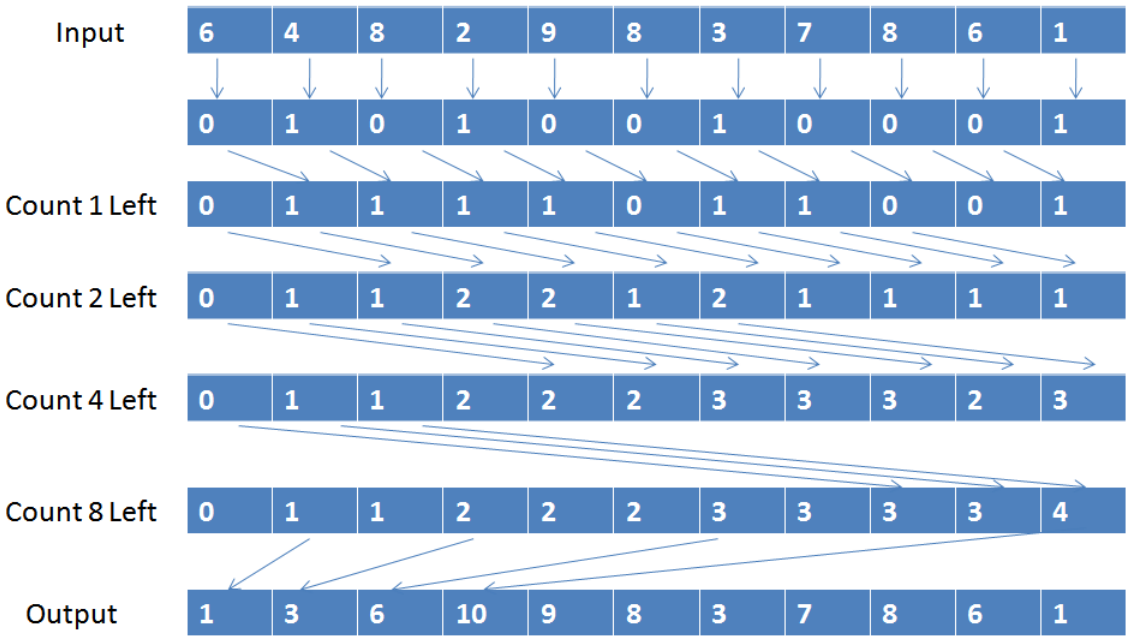

Figure 4.3: Iteratively counting number of objects in result set.

```
1  kernel void scan_index(int metaData[], int twotoi, int input[][], out
       int results_index<>)
2  {
3    int2 cindex = instance().xy;
4    int logicalIndex = (metaData[0]*cindex.y)+cindex.x-twotoi;
5    int val = input[cindex.y][cindex.x];
6
7    if (logicalIndex >= metaData[1])
8      return;
9
10   if (logicalIndex >= 0){
11     cindex.x = logicalIndex % metaData[0];
12     cindex.y = logicalIndex / metaData[0];
13     val += input[cindex.y][cindex.x];
14   }
15   results_index = val;
16 }
```

Listing 4.10: ATI CAL Kernel for Result Set Filtering Scan

After performing this multipass counting kernel log n times, each record knows how many valid distances are present before them. The value at the very right of the stream indicates how many objects there are in the result set, and hence the length of the compacted output. To get size of result set kernel listed in listing 4.11 is invoked.

```
1 kernel void result_set_size(int metaData[],int results_index[][],out
      int count<>)
2 {
3   int2 index;
4   index.x = (metaData[1]-1) %  metaData[0];
5   index.y = (metaData[1]-1) / metaData[0];
6   count = results_index[index.y][index.x];
7 }
```

Listing 4.11: ATI CAL Kernel for Obtaining Result Set Size

If result set size greater than zero, a new stream where first number of result set size elements contains indexes of objects that are in result set is computed through a scatter operation. As in this step each value in the stream holds number of valid distances to left of it (counting it self also), its position on this new stream is its value minus one. Kernel implementing scatter operation is listed in listing 4.12

```
1 kernel void filter_results(int metaData[],float radius,float
     distance<>,int results_index<>,out int filtered_index[][])
2 {
3   int2 index = instance().xy;
4   int inputlogicalIndex;
5   int outputlogicalIndex;
6   if (radius >= distance) {
7     inputlogicalIndex = (metaData[0]*index.y)+index.x;
8
9     if (inputlogicalIndex >= metaData[1])
10      return;
11
12    outputlogicalIndex = results_index-1;
13    index.x = outputlogicalIndex %  metaData[0];
14    index.y = outputlogicalIndex / metaData[0];
```

```
15
16      filtered_index[index.y][index.x] = inputlogicalIndex;
17    }
18 }
```

Listing 4.12: ATI CAL Kernel for Filtering Result set

Now we have a stream which contain indexes of objects which are in the result set, a new stream with appropriate size is created to retrieve index and computed distance to query object. Kernel listed in listing 4.13 is used to copy results back to system memory.

```
1  kernel void copy_filtered_results(int metaData[],float distance[][],
       int results_index[][],out float2 resultset<>)
2  {
3    float2 val;
4
5    int cindex = ((instance().y*metaData[0])+instance().x)*4;
6    int rindex = results_index[cindex/metaData[0]][cindex % metaData
         [0]];
7    int x = rindex % metaData[0];
8    int y = rindex / metaData[0];
9    val.x = (float)rindex;
10   val.y = distance[y][x];
11   resultset = val;
12 }
```

Listing 4.13: ATI CAL Kernel for copying Filtered Result set

Chapter 5

Experiment Results

Experimental data are collected using a system which had 2 graphics cards; ATI Radeon 4870x2 (2GB) and ATI Radeon 5870 (1GB), 6GB of system memory with Intel i7 cpu. Details of system configuration is given in table 5.1 Implementation is done on C++ and compiled with all optimization flags enabled. In order to utilize all the multi-threading capabilities of cpu, cpu versions of algorithms are run in 8 (which produced the best performance) different threads. In these tests, measurements are performed by following steps:

1. **Initialization:** objects,index structures and queries are loaded.
2. **Warming Run:** before measuring execution time, a warming run for the query is performed.
3. **Query Execution:** 1000 queries are repeatedly executed to minimize measurement errors and elapsed time is reported.

The synthetic data used in these tests consists of randomly generated vectors with varying dimensions (16,32,48,64,80,96,112,128,144 and 160). Each dimension is random coordinate value uniformly distributed over the range $[0.0 - 1.0]$. The object collection on which similarity queries were executed consisted of 2^{20} vectors up to 10×2^{20} vectors. Measurements of timings are grouped into two test

Test Hardware	
Processor	Intel Core i7-920 (Bloomfield) 2.66 GHz, 8 MB L3 Cache, power-saving settings disabled
Motherboard	LANPARTY DK X58-T3eH6
Memory	Corsair Dominator 6GB (3 x 2GB) DDR3-1600 8-8-8-24 @ 1,600 MHz
Graphics Cards	ATI Radeon HD 4870x2 ATI Radeon HD 5870
System Software and Drivers	
Operating System	Microsoft Windows 7 Ultimate x64
Graphics Driver	AMD Catalyst 9.12

Table 5.1: System configuration of Test Hardware

	Test Set 1		Test Set 2	
Run#	Dimension	Object Count	Dimension	Object Count
1	16	1048576	16	1048576
2	32	1048576	16	2097152
3	48	1048576	16	3145728
4	64	1048576	16	4194304
5	80	1048576	16	5242880
6	96	1048576	16	6291456
7	112	1048576	16	7340032
8	128	1048576	16	8388608
9	144	1048576	16	9437184
10	160	1048576	16	10485760

Table 5.2: Number of objects and dimension sizes used in measurements.

sets and named as test set 1 and test set 2. Test set 1 aims to measure effect of dimensionality on execution times, by taking execution times with same object count (2^{20}) and varying dimensions. Test set 2 aims to measure effect of object count on execution times, by taking execution times with same dimensionality (16) and varying object count. Table 5.2 shows object counts and dimension sizes used in each test set

Only results of ATI CAL implementation is reported in this work, as Brook+ and OpenCL implementation performances were similar, as they are built on ATI CAL framework in implementations provided by ATI.

These test sets are measured against various implementations. First GPU implementations where distance computations were done in GPU, distance values returned to system memory and result set filtering was done on CPU were measured. Then in order to see effect of GPU to CPU data transfers, same tests are repeated and execution times are measured for the modified implementation where there were no distance value transfer from GPU to system memory. Lastly same tests are repeated with implementation where filtering performed on GPU and only result set is transferred from GPU to system memory.

In the following sub-sections we report results of theses experiments.

5.1 Comparison of implementations with Result Set Filtering on CPU

In these tests, aim was to measure speedups obtained by GPU utilization in distance computation. Implementations used in this test compute distance values on the GPU and reports back query to object distance for each object. Distance function was selected to be euclidean distance of query and object vectors. Filtering of distances are done on CPU side.

D	N	Linear Scan	KVP	CAL	KVP CAL
16	1048576	59.11	35.25	20.16	22.18
32	1048576	101.13	36.87	21.19	21.94
48	1048576	140.81	37.18	22.18	21.99
64	1048576	182.76	30.53	22.67	21.92
80	1048576	223.68	32.25	23.95	22.06
96	1048576	264.41	36.11	25.09	22.13
112	1048576	301.96	35.95	27.31	19.54
128	1048576	355.24	37.84	27.99	20.86
144	1048576	385.97	38.17	30.78	20.45
160	1048576	427.46	39.66	30.81	20.03

Table 5.3: Execution times in seconds for 1000 radius queries on object set size of 2^{20} vectors, with varying vector dimensions. Result set filtering performed on CPU.

In order to see effects of object dimension size and object collection size two sets of different tests were performed. In test set 1, dimension of the vectors were changed between 16 to 160, by increments of 16, and number of objects are kept constant at 2^{20}. Table 5.3 shows measured timings for test set 1, figure 5.1 shows results as chart. Figure 5.2 shows speed up factors for each implementation compared to CPU brute force search.

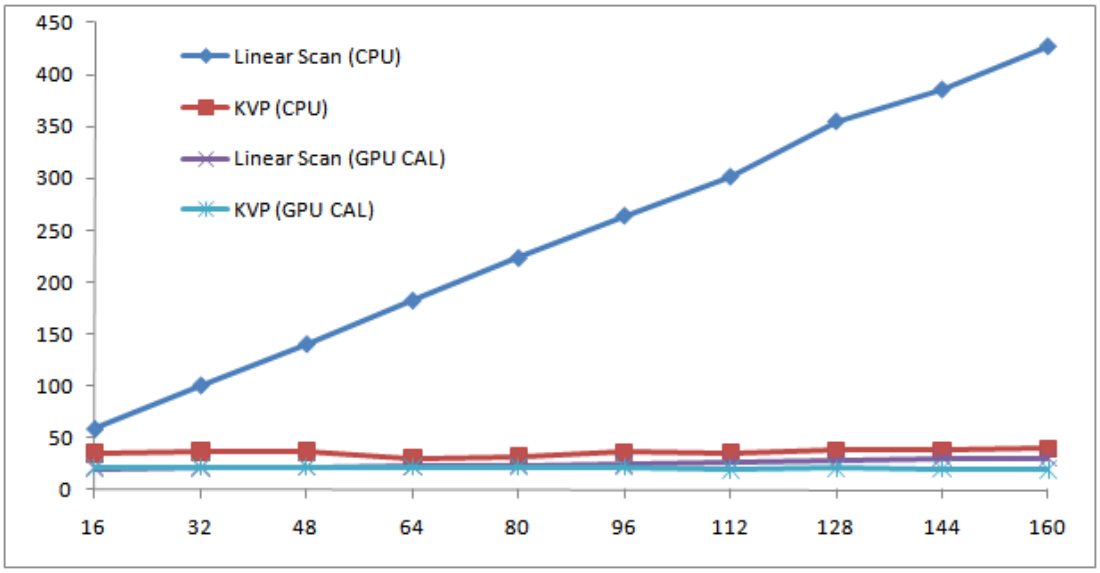

Figure 5.1: Execution times in seconds for 1000 radius queries on 2^{20} vectors, with varying vector dimensions. Result set filtering performed on CPU.

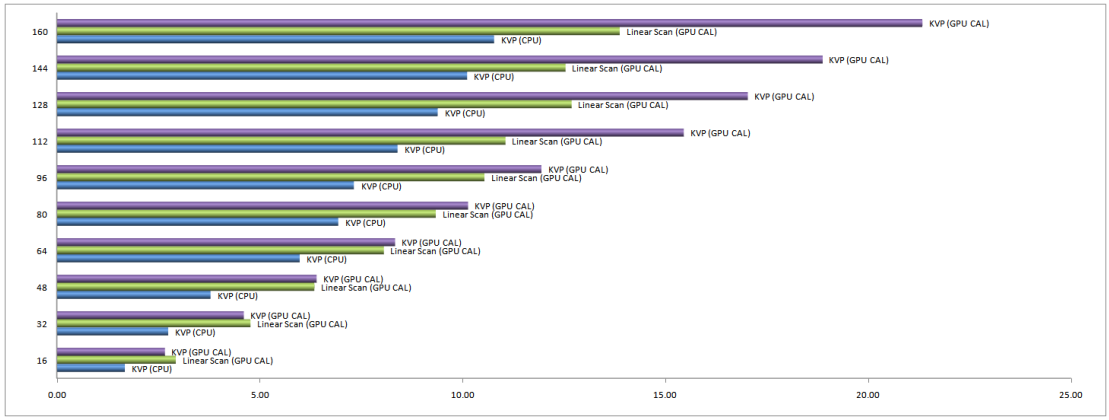

Figure 5.2: Relative speeds of implementations for test set 1, when result set filtering is performed on CPU.

Results show that as the number of dimensions increase, GPU versions of the algorithms perform considerable better from CPU versions. While in lower

dimensions speedup factor is only 2.66, as dimension size increases the speed up increases. In the test performed using 1048576 vectors of 160 dimensions, speed up factor was 21.23. This is in accord with the expectation that as distance function gets computationally intensive, gains from GPU utilization increases. Both CPU and GPU implementation execution times increase linearly, as expected. Yet GPU version of KVP algorithm has best slope, scaling better. Also it is worth to note that KVP algorithm is slightly slower in the test performed using 16 dimensioned vectors from GPU implementation of brute force scan. As dimensions increase GPU implementation of KVP outperforms GPU version of brute force scan by speed up factor of 1.5.

D	N	Linear Scan	KVP	CAL	KVP CAL
16	1048576	59.26	35.33	20.15	22.13
16	2097152	119.81	73.84	38.86	43.11
16	3145728	180.13	104.43	57.83	63.47
16	4194304	241.03	156.87	76.51	84.33
16	5242880	309.31	187.57	95.55	103.59
16	6291456	376.38	245.77	114.53	124.93
16	7340032	436.79	245.03	133.38	144.82
16	8388608	495.22	297.82	152.26	165.41
16	9437184	557.72	346.96	171.29	186.45
16	10485760	613.90	362.56	190.18	188.37

Table 5.4: Execution times in seconds for 1000 radius queries on vectors with 16 dimensions and varying number of vectors. Result set filtering performed on CPU.

In order to see effects of object collection size another set of different tests are performed. In test set 2, dimension of the vectors are kept constant at 16 and number of objects are incremented by 2^{20}. Table 5.4 shows measured timings for test set 2, figure 5.3 shows results as chart. Figure 5.4 shows speed up factors for each implementation compared to CPU brute force search.

Results show that as number of of objects increase, GPU versions of the algorithms still perform better but speed up factor, although slightly increases as number of objects increase, is nearly same for all object collection size. Both CPU and GPU implementation execution times increase linearly, as expected, but slope of GPU implementations was higher than test set 1 results. Later experiments

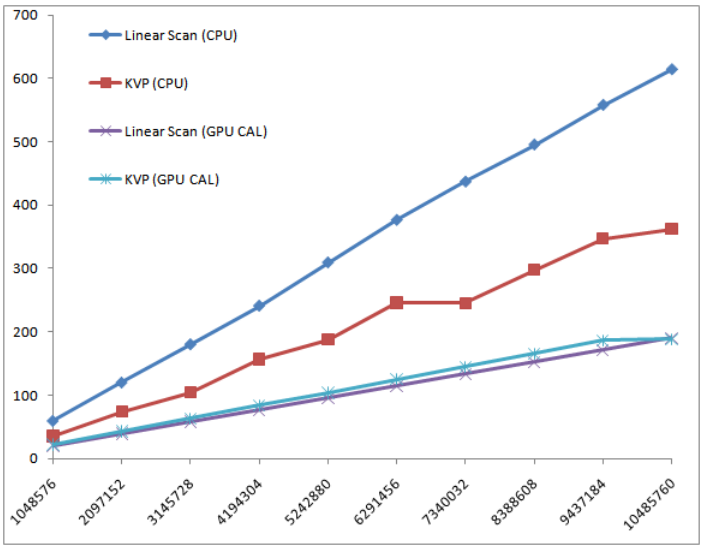

Figure 5.3: Execution times in seconds for 1000 radius queries on vectors with 16 dimensions and varying number of vectors. Result set filtering performed on CPU.

showed that this was due to system memory to graphic card memory distance value transfers. In test set 1 only dimensions were changing which did not effect number of distance values transferred from graphic card memory to system memory. Second set of tests used varying number of objects, thus increasing number of distances to be transferred from graphic card memory to system memory.

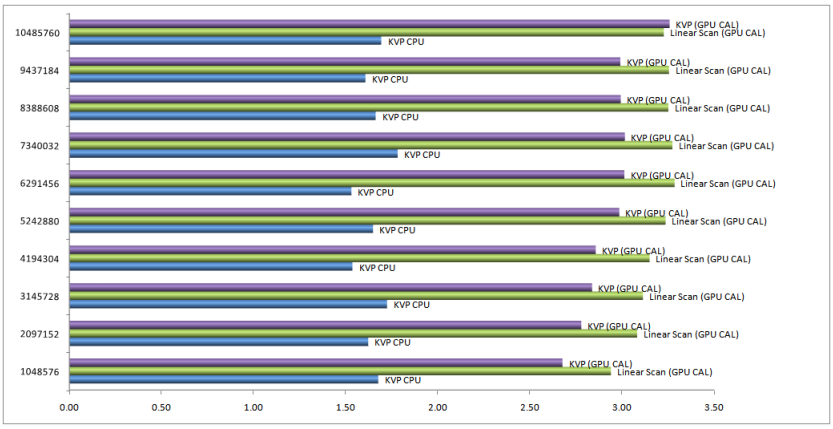

Figure 5.4: Relative speeds of implementations for test set 2, when result set filtering is performed on CPU.

5.2 Performance Overhead of Data Transfers from GPU to CPU

As it can be seen results of previous tests, memory transfers from GPU to CPU has quite impact on execution times. The tests reported in this section are performed to see how great this impact was.

D	N	Linear Scan	KVP	CAL	KVP CAL
16	1048576	59.11	35.25	2.17	2.54
32	1048576	101.13	36.87	3.81	2.70
48	1048576	140.81	37.18	5.21	2.87
64	1048576	182.76	30.53	6.76	2.90
80	1048576	223.68	32.25	8.23	3.06
96	1048576	264.41	36.11	9.41	3.21
112	1048576	301.96	35.95	11.27	3.20
128	1048576	355.24	37.84	12.54	3.28
144	1048576	385.97	38.17	14.09	3.35
160	1048576	427.46	39.66	14.78	3.60

Table 5.5: Execution times in seconds for 1000 radius queries on object set size of 2^{20} vectors, with varying vector dimensions, no result set fetching.

In order to measure effect of memory transfers from GPU to CPU, implementations were modified so as leave distances values on the graphic card memory. Other than distance value fetch code from graphic memory, everything in the code left same, which assures that GPU still computes the distance values. After this modification same sets of tests performed. Table 5.5 shows measured timings for test set 1, figure 5.5 shows results as chart. Figure 5.6 shows speed up factors for each implementation compared to CPU brute force search.

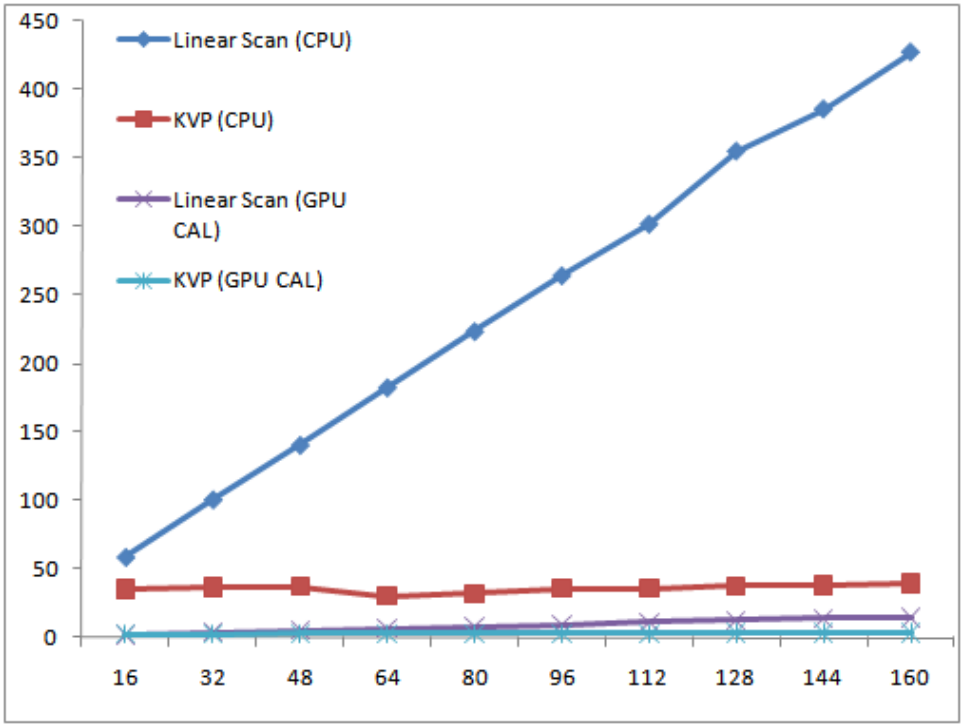

Figure 5.5: Execution times in seconds for 1000 radius queries on object set size of 2^{20} vectors, with varying vector dimensions, no result set fetching.

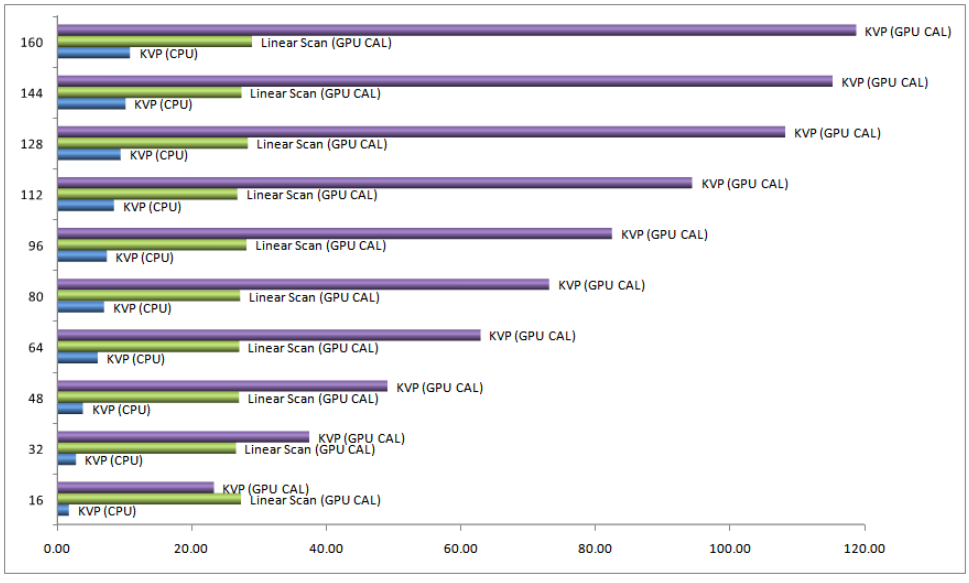

Figure 5.6: Relative speeds of implementations for test set 1, no result set fetching.

When we compare these measurement of execution times with the implementations that fetch distance values from GPU memory, we can compute memory transfer overheads from GPU to system memory. By dividing size of data transferred to time difference data transfer rate is calculated. Data transfer rates is shown in Table 5.6.

D	N	Data (MB)	Time(sec.)	Transfer Rate (MB/sec)	% Execution
16	1048576	4,000	17.99	222.3213	89.25%
32	1048576	4,000	17.39	230.0770	82.03%
48	1048576	4,000	16.96	235.8018	76.49%
64	1048576	4,000	15.91	251.4362	70.18%
80	1048576	4,000	15.72	254.5087	65.62%
96	1048576	4,000	15.68	255.1284	62.50%
112	1048576	4,000	16.03	249.5135	58.71%
128	1048576	4,000	15.45	258.8953	55.20%
144	1048576	4,000	16.69	239.6985	54.22%
160	1048576	4,000	16.03	249.4988	52.04%
16	1048576	4,000	18.00	222.2045	89.32%
16	2097152	8,000	35.61	224.6259	91.64%
16	3145728	12,000	53.48	224.3881	92.48%
16	4194304	16,000	71.05	225.2083	92.86%
16	5242880	20,000	89.02	224.6768	93.16%
16	6291456	24,000	106.92	224.4599	93.36%
16	7340032	28,000	124.67	224.5862	93.47%
16	8388608	32,000	142.46	224.6204	93.56%
16	9437184	36,000	160.41	224.4290	93.65%
16	10485760	40,000	178.19	224.4748	93.70%

Table 5.6: Data Transfer rate and percentage of time used in data transfers.

Analysis of data shows data transfer rates are below theoretical value. According to PCI Express Base 2.0 specification on 15 January 2007 the per-lane throughput is 500 MB/s. This means a 16-lane PCI connector which is supported by graphic cards, can support throughput up to 8 GB/s aggregate. Observed maximum transfer rate was only 259MB/sec, which is far below theoretical value. In order to understand reason for slow data transfers, transfer rate is measured with a utility program provided by ATI, in order to identify non compliant or fault motherboard or some other hardware issue. Measuring with utility program

from ATI confirmed that theoretical limit can be achieved for large data transfers. Thus it is concluded that frameworks used in implementation causes an overhead per transfer, and small data transfers are effected most.

D	N	Linear Scan	KVP	CAL	KVP CAL
16	1048576	59.26	35.33	2.15	2.53
16	2097152	119.81	73.84	3.25	4.00
16	3145728	180.13	104.43	4.35	5.27
16	4194304	241.03	156.87	5.47	6.80
16	5242880	309.31	187.57	6.54	8.31
16	6291456	376.38	245.77	7.61	10.11
16	7340032	436.79	245.03	8.71	10.75
16	8388608	495.22	297.82	9.80	12.51
16	9437184	557.72	346.96	10.88	14.19
16	10485760	613.90	362.56	11.98	15.17

Table 5.7: Execution times in seconds for 1000 radius queries on vectors with 16 dimensions and varying number of vectors, no result set fetching..

Same implementation is measured using test set 2. Table 5.7 shows measured timings for test set 2, figure 5.7 shows results as chart. Figure 5.8 shows speed up factors for each implementation compared to CPU brute force search.

Analysis of data shows again that if memory transfers were not such a bottleneck further speed ups are possible. Test results show speed up factors up 50 times, lower than previous maximum speed ups measured by test set 1 data, which confirm the intuition that as kernels get more computationally intensive, benefits of using GPU increases. It is also worth noting that as number of objects increase, number of kernel threads increase an a slight penalty in performance occurs.

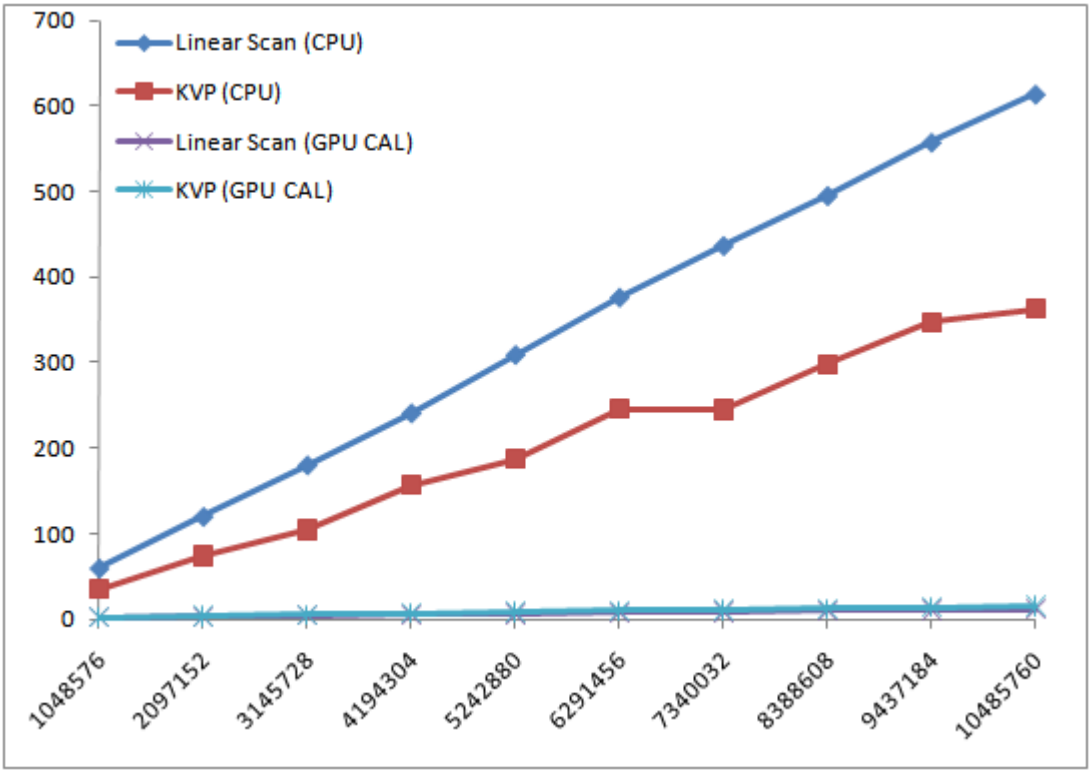

Figure 5.7: Execution times in seconds for 1000 radius queries on vectors with 16 dimensions and varying number of vectors, no result set fetching..

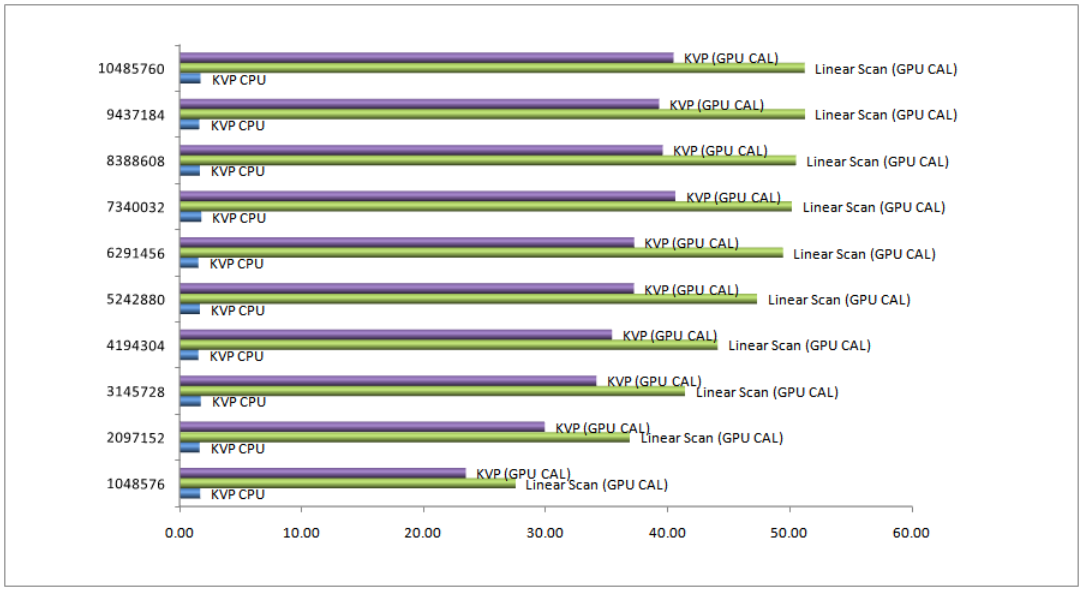

Figure 5.8: Relative speeds of implementations for test set 2, no result set fetching.

5.3 Comparison of implementations with Result Set Filtering on GPU

If we look at table 5.6, we see that nearly %90 time is used for data transfers. So it is expected that further acceleration is possible if this situation was remedied. Since we had no control over frameworks used and PCI bus hardware, we tried to reduce data size transferred. By performing filtering of distance values that are greater than query radius on GPU side, we were able to reduce data transferred at the expense of more computationally expensive filtering.

D	N	Linear Scan	KVP	CAL	KVP CAL
16	1048576	59.11	35.25	13.55	14.01
32	1048576	101.13	36.87	14.94	14.10
48	1048576	140.81	37.18	16.26	14.10
64	1048576	182.76	30.53	16.82	14.12
80	1048576	223.68	32.25	18.16	14.16
96	1048576	264.41	36.11	19.15	14.53
112	1048576	301.96	35.95	21.32	14.49
128	1048576	355.24	37.84	22.03	14.44
144	1048576	385.97	38.17	24.10	15.71
160	1048576	427.46	39.66	24.72	16.02

Table 5.8: Execution times in seconds for 1000 radius queries on object set size of 2^{20} vectors, with varying vector dimensions, GPU result set filtering.

D	N	Linear Scan	KVP	CAL	KVP CAL
16	1048576	59.26	35.33	13.49	13.91
16	2097152	119.81	73.84	19.28	20.16
16	3145728	180.13	104.43	28.21	29.31
16	4194304	241.03	156.87	35.37	37.38
16	5242880	309.31	187.57	47.33	49.67
16	6291456	376.38	245.77	56.45	59.67
16	7340032	436.79	245.03	62.59	65.28
16	8388608	495.22	297.82	71.41	74.70
16	9437184	557.72	346.96	82.97	87.25
16	10485760	613.90	362.56	92.07	96.10

Table 5.9: Execution times in seconds for 1000 radius queries on vectors with 16 dimensions and varying number of vectors, GPU result set filtering.

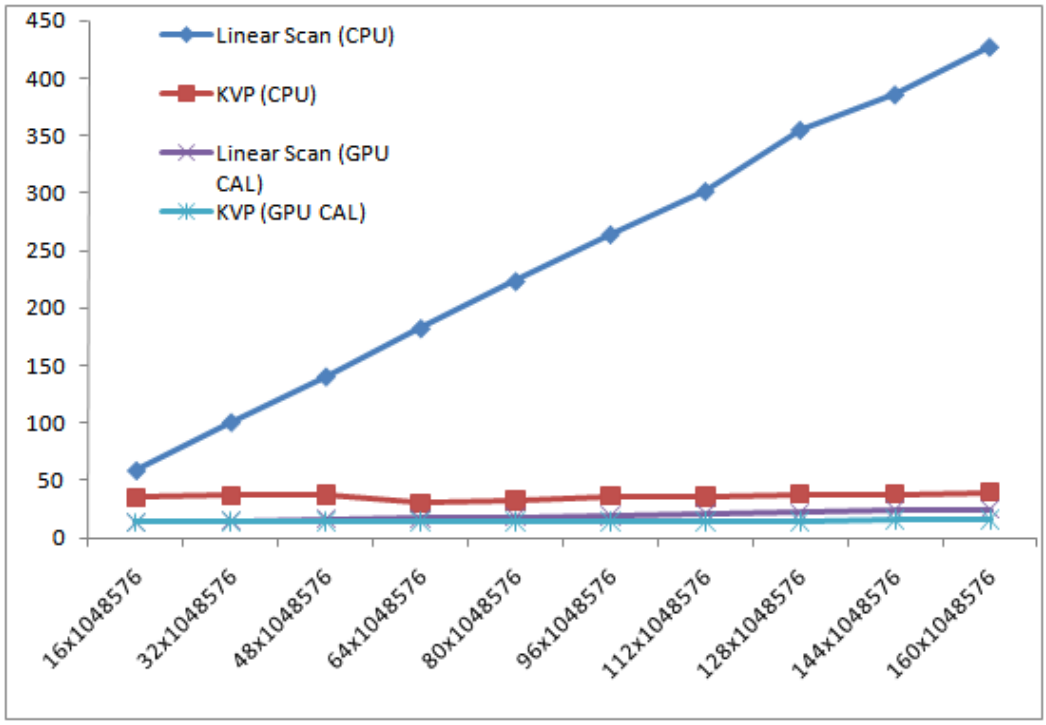

Figure 5.9: Execution times for 1000 radius queries on object set size of 2^{20} vectors, with varying vector dimensions, GPU result set filtering.

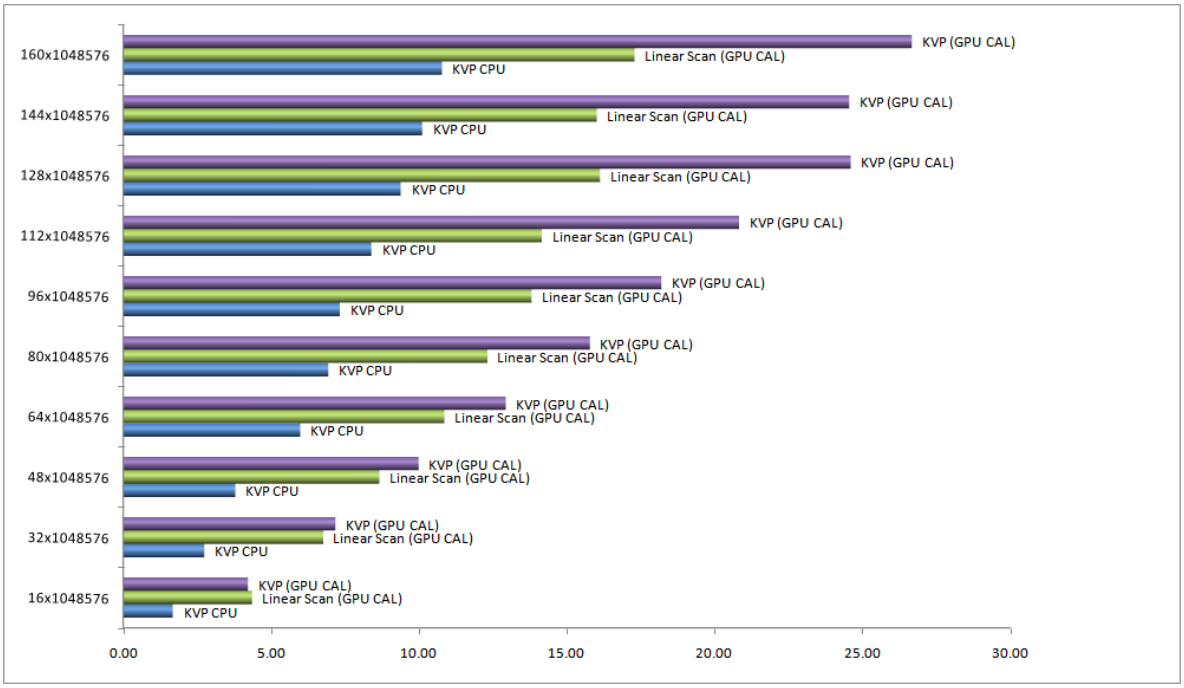

Figure 5.10: Relative speeds of implementations for test set 1, GPU result set filtering.

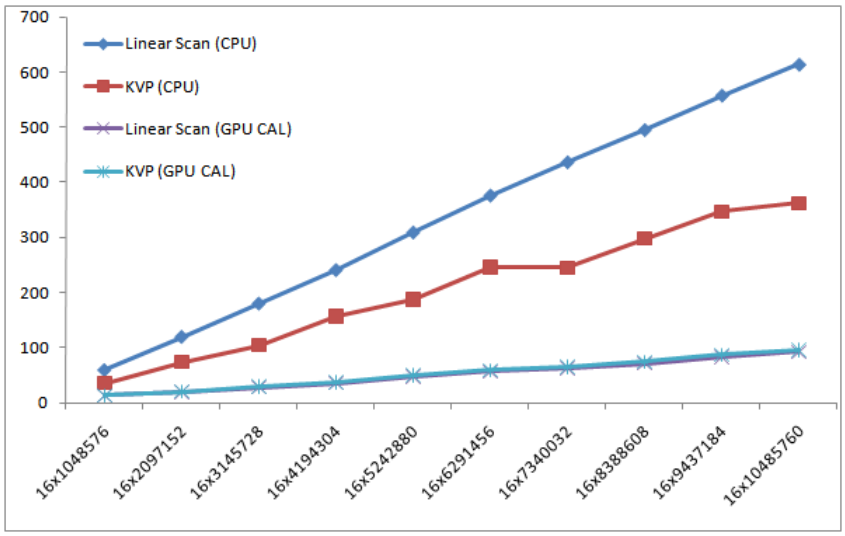

Figure 5.11: Execution times for 1000 radius queries on vectors with 16 dimensions and varying number of vectors, GPU result set filtering.

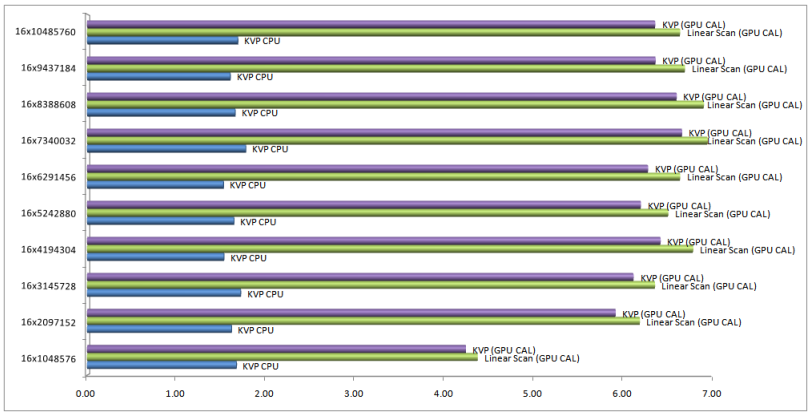

Figure 5.12: Relative speeds of implementations for test set 2, GPU result set filtering.

Same sets of tests are performed and results are presented in Table 5.8 which shows measured timings for test set 1, figure 5.9 shows results as chart. Figure 5.10 shows speed up factors for each implementation compared to CPU brute force search. Table 5.9 shows measured timings for test set 2, figure 5.11 shows results as chart. Figure 5.12 shows speed up factors for each implementation compared to CPU brute force search.

Results show that as number of dimensions increase, GPU versions of the algorithms perform considerable better from CPU versions in accordance with

previous tests. While in lower dimensions speedup factor is only 4.36, as dimension size increases speed up increases. In tests performed using 1048576 vectors of 160 dimensions, speed up factor was 26.68. This was an improvement over implementing filtering in CPU, which yielded speed up factor of 21.23.

Chapter 6

Conclusion

The field of GPGPU computing is advancing quickly. Many GPGPU algorithms continue to be developed for a wide range of problems, from physical simulations to data mining. Current graphics APIs, and GPGPU languages, provide a fast computation platform, hiding much of the complexity of parallel execution.

GPUs are growing more general and as high-level languages and toolkits become available, low-level GPGPU programming is becoming obsolete. Progress of graphic card architecture suggest next generation of graphic cards to be more suitable to general purpose computation. High-level shader languages provides eases task of GPU developers, and languages like BrookGPU and standardization efforts like OpenCL hold similar promise for non-graphics developers who wish to harness the power of GPUs.

From a general perspective, GPUs may be seen as the first generation of commodity data-parallel co-processors. Their rapidly increasing computational capacity that is growing faster than CPUs, make them an attractive platform for domain specialized, data-parallel computing. Benefits of this platform can be leveraged further by performing large-scale GPGPU computing with large clusters of GPU-equipped computers.

At the same time, CPU vendors are aggressively pursuing multi-core designs,

including a heterogeneous example in the Cell processor produced by IBM, Sony, and Toshiba. The tiled architecture of Cell provides a dense computational fabric well suited to the stream programming model, similar in many ways to GPUs but oriented toward running fewer threads with more available resources than the very large number of fine-grained, lightweight threads on the GPU. Mainstream CPU vendors like Intel and AMD are continually increasing core numbers to improve performance as opposed to previous approach of making them faster by increasing operating frequencies.

All these advances in computer hardware provide an opportunity for developing new algorithms or adaptation of current algorithms so that one can utilize these emerging hardware. In the light of this facts, we decided a computationally intensive task like similarity searching can benefit from advances in graphics card hardware, more generally architectures that emphasize parallelism in computation. Our work confirms this intuition.

In this thesis, we have presented an approach for accelerating similarity search queries using GPUs. A number of implementations with practical improvements to data structures and algorithms for similarity searching in metric spaces in GPUs is presented. We have evaluated the efficiency of these implementations through a number of empirical analyses.

We provided implementations for brute force search and KVP algorithms for CPU and GPU. When compared with CPU implementation of brute force search, GPU version of brute force search was faster 17 times. GPU version of KVP algorithm achieved speed ups up to 27 times.

We showed that similarity search implementations can benefit significantly from GPU utilization. Experimental results show that current graphic card processors extremely powerful. Although hindered by system memory to graphic card memory data transfers and overhead incurred by GPGPU frameworks, implementations provided in this work provided speedups up to 27 times when compared with optimized, multi threaded CPU implementation. We believe this speed up can be greater for applications that requires more computationally intensive distance function than used in this work.

We have showed that data transfer from graphic memory to system memory (and vice versa) incurs significant impact on execution time. We have provided a solution to reduce data transfers in processing similarity search queries.

The challenge in this work was to adapt existing algorithms that were designed with the CPU architecture in mind, to graphic cards execution architecture. Also another problem was the lack of tools like debuggers and profilers for GPGPU environment. Although GPGPU computing is maturing, it is completely established. Thus bugs, and lack of documentation on part of vendors that produces graphic cards made some problems harder to solve.

As future work, same work can be implemented on emerging heterogeneous systems such as the Sony Playstation 3, which joins a Cell processor and a modern GPU with a high-bandwidth bus, present interesting opportunities and challenges.

Bibliography

[1] Microsoft shader debugger. Available at `http://msdn.microsoft.com/library/default.asp?url=/library/en-us/directx9c/directx/graphics/Tools/ShaderDebugger.asp`, 2005.

[2] Graphic remedy gdebugger. Available at `http://www.gremedy.com/`, 2006.

[3] S. Arya and D. M. Mount. Algorithm for fast vector quantization. In J. A. Storer and M. Cohn, editors, *Proceedings DCC93 (IEEE Data Compression Conference)*, pages 381–390, Snowbird, UT, USA, March 1993.

[4] B. Baxter. The image debugger. Available at `http://www.billbaxter.com/projects/imdebug/`, 2006.

[5] K. S. Beyer, J. Goldstein, R. Ramakrishnan, and U. Shaft. When is "nearest neighbor" meaningful? In *ICDT '99: Proceedings of the 7th International Conference on Database Theory*, pages 217–235, London, UK, 1999. Springer-Verlag.

[6] D. Blythe. The direct3d 10 system. *ACM Trans. Graph.*, 25(3):724–734, 2006.

[7] C.-A. Bohn. Kohonen feature mapping through graphics hardware. In *In Proceedings of Int. Conf. on Compu. Intelligence and Neurosciences*, pages 64–67, 1998.

[8] J. Bolz, I. Farmer, E. Grinspun, and P. Schröoder. Sparse matrix solvers on the gpu: conjugate gradients and multigrid. *ACM Trans. Graph.*, 22(3):917–924, 2003.

[9] T. Bozkaya and M. Ozsoyoglu. Distance-based indexing for high-dimensional metric spaces. In *SIGMOD '97: Proceedings of the 1997 ACM SIGMOD international conference on Management of data*, pages 357–368, New York, NY, USA, 1997. ACM.

[10] S. Brin. Near neighbor search in large metric spaces. In *The VLDB Journal*, pages 574–584, 1995.

[11] I. Buck. Taking the plunge into gpu computing. In M. Pharr, editor, *GPU Gems 2*, pages 509–519. Addison Wesley, 2005.

[12] I. Buck, T. Foley, D. Horn, J. Sugerman, K. Mike, and H. Pat. Brook for gpus: Stream computing on graphics hardware. In *ACM Transactions on Graphics (Proceedings of SIGGRAPH 2004)*, volume 23, pages 777–786, 2004.

[13] I. Buck and T. Purcell. A toolkit for computation on gpus. In R. Fernando, editor, *GPU Gems*, pages 621–636, 2004.

[14] W. A. Burkhard and R. M. Keller. Some approaches to best-match file searching. *Commun. ACM*, 16(4):230–236, April 1973.

[15] E. Chávez, J. L. Marroquín, and R. Baeza-Yates. Spaghettis: An array based algorithm for similarity queries in metric spaces. In *SPIRE '99: Proceedings of the String Processing and Information Retrieval Symposium & International Workshop on Groupware*, page 38, Washington, DC, USA, 1999. IEEE Computer Society.

[16] E. Chávez, J. L. Marroquín, and G. Navarro. Fixed queries array: A fast and economical data structure for proximity searching. *Multimedia Tools Appl.*, 14(2):113–135, 2001.

[17] P. Ciaccia, M. Patella, and P. Zezula. M-tree: An efficient access method for similarity search in metric spaces. In *VLDB '97: Proceedings of the 23rd International Conference on Very Large Data Bases*, pages 426–435, San Francisco, CA, USA, 1997. Morgan Kaufmann Publishers Inc.

[18] C. Çelik. *New Approaches to Similarity Searching in Metric Spaces*. PhD thesis, University of Maryland, 2006.

[19] J. N. England. A system for interactive modeling of physical curved surface objects. *SIGGRAPH Comput. Graph.*, 12(3):336–340, 1978.

[20] U. Erra. Toward real time fractal image compression using graphics hardware. pages 723–728, 2005.

[21] C. Faloutsos, R. Barber, M. Flickner, J. Hafner, W. Niblack, D. Petkovic, and W. Equitz. Efficient and effective querying by image content. *Journal of Intelligent Information Systems*, 3(3/4):231–262, 1994.

[22] C. Faloutsos and K.-I. Lin. Fastmap: a fast algorithm for indexing, data-mining and visualization of traditional and multimedia datasets. In *SIGMOD '95: Proceedings of the 1995 ACM SIGMOD international conference on Management of data*, pages 163–174, New York, NY, USA, 1995. ACM.

[23] T. Foley and J. Sugerman. Kd-tree acceleration structures for a gpu raytracer. In *HWWS '05: Proceedings of the ACM SIGGRAPH/EUROGRAPHICS conference on Graphics hardware*, pages 15–22, New York, NY, USA, 2005. ACM.

[24] V. Gaede and O. Günther. Multidimensional access methods. *ACM Computing Surveys*, 30(2):170–231, 1998.

[25] N. Goodnight, C. Woolley, G. Lewin, D. Luebke, and G. Humphreys. A multigrid solver for boundary value problems using programmable graphics hardware. In *HWWS '03: Proceedings of the ACM SIGGRAPH/EUROGRAPHICS conference on Graphics hardware*, pages 102–111, Aire-la-Ville, Switzerland, Switzerland, 2003. Eurographics Association.

[26] N. Govindaraju, J. Gray, R. Kumar, and D. Manocha. Gputerasort: high performance graphics co-processor sorting for large database management. In *SIGMOD '06: Proceedings of the 2006 ACM SIGMOD international conference on Management of data*, pages 325–336, New York, NY, USA, 2006. ACM.

[27] N. K. Govindaraju, M. Henson, M. C. Lin, and D. Manocha. Interactive visibility ordering and transparency computations among geometric primitives in complex environments. In *I3D '05: Proceedings of the 2005 symposium on Interactive 3D graphics and games*, pages 49–56, New York, NY, USA, 2005. ACM.

[28] N. K. Govindaraju, B. Lloyd, W. Wang, M. Lin, and D. Manocha. Fast computation of database operations using graphics processors. In *SIGGRAPH '05: ACM SIGGRAPH 2005 Courses*, page 206, New York, NY, USA, 2005. ACM.

[29] N. K. Govindaraju, N. Raghuvanshi, and D. Manocha. Fast and approximate stream mining of quantiles and frequencies using graphics processors. In *SIGMOD '05: Proceedings of the 2005 ACM SIGMOD international conference on Management of data*, pages 611–622, New York, NY, USA, 2005. ACM.

[30] A. Greß, M. Guthe, and R. Klein. Gpu-based collision detection for deformable parameterized surfaces. *Computer Graphics Forum*, 25(3):497–506, Sept. 2006.

[31] E. Greß and G. Zachmann. Gpu-abisort: Optimal parallel sorting on stream architectures. In *In Proceedings of the 20th IEEE International Parallel and Distributed Processing Symposium (IPDPS 06) (Apr*, page 45, 2006.

[32] M. Harris. Mapping computational concepts to gpus. In *SIGGRAPH '05: ACM SIGGRAPH 2005 Courses*, page 50, New York, NY, USA, 2005. ACM.

[33] M. Harris and I. Buck. Gpu flow control idioms. In M. Pharr, editor, *GPU Gems 2*, pages 547–555. Addison Wesley, 2005.

[34] M. J. Harris. Analysis of error in a cml diffusion operation. Technical report, 2002.

[35] M. J. Harris, G. Coombe, T. Scheuermann, and A. Lastra. Physically-based visual simulation on graphics hardware. In *HWWS '02: Proceedings of the ACM SIGGRAPH/EUROGRAPHICS conference on Graphics hardware*,

pages 109–118, Aire-la-Ville, Switzerland, Switzerland, 2002. Eurographics Association.

[36] J. Hensley, T. Scheuermann, G. Coombe, M. Singh, and A. Lastra. Fast summed-area table generation and its applications. *Computer Graphics Forum*, 24:547–555, 2005.

[37] D. W. Hillis and G. L. Steele. Data parallel algorithms. *Commun. ACM*, 29(12):1170–1183, December 1986.

[38] G. R. Hjaltason and H. Samet. Index-driven similarity search in metric spaces (survey article). *ACM Trans. Database Syst.*, 28(4):517–580, 2003.

[39] G. R. Hjaltason and H. Samet. Properties of embedding methods for similarity searching in metric spaces. *IEEE Trans. Pattern Anal. Mach. Intell.*, 25(5):530–549, May 2003.

[40] M. Hopf and T. Ertl. Hardware based wavelet transformations, 1999.

[41] D. Horn. Stream reduction operations for gpgpu applications. In M. Pharr, editor, *GPU Gems 2*, pages 573–589. Addison Wesley, 2005.

[42] G. Hristescu and M. Farach. Cluster-preserving embedding of proteins. Technical report, 1999.

[43] T. Jansen, B. von Rymon-Lipinski, N. Hanssen, and E. Keeve. Fourier volume rendering on the gpu using a split-stream-fft. In *VMV*, pages 395–403, 2004.

[44] C. T. Jr., A. J. M. Traina, B. Seeger, and C. Faloutsos. Slim-trees: High performance metric trees minimizing overlap between nodes. In *EDBT*, pages 51–65, 2000.

[45] G. Kedem and Y. Ishihara. Brute force attack on unix passwords with simd computer. In *SSYM'99: Proceedings of the 8th conference on USENIX Security Symposium*, pages 8–8, Berkeley, CA, USA, 1999. USENIX Association.

[46] P. Kipfer, M. Segal, and R. Westermann. Uberflow: a gpu-based particle engine. In *HWWS '04: Proceedings of the ACM SIGGRAPH/EUROGRAPHICS conference on Graphics hardware*, pages 115–122, New York, NY, USA, 2004. ACM.

[47] A. Kolb and N. Cuntz. Dynamic particle coupling for gpu-based fluid simulation. *Proc. 18th Symposium on Simulation Technique*, pages 722–727, 2005.

[48] F. Korn, N. Sidiropoulos, C. Faloutsos, E. Siegel, and Z. Protopapas. Fast nearest neighbor search in medical image databases. In *The VLDB Journal*, pages 215–226, 1996.

[49] J. Krüger and R. Westermann. Linear algebra operators for gpu implementation of numerical algorithms. In *SIGGRAPH '05: ACM SIGGRAPH 2005 Courses*, page 234, New York, NY, USA, 2005. ACM.

[50] A. E. Lefohn, J. M. Kniss, C. D. Hansen, and R. T. Whitaker. A streaming narrow-band algorithm: interactive computation and visualization of level sets. In *SIGGRAPH '05: ACM SIGGRAPH 2005 Courses*, page 243, New York, NY, USA, 2005. ACM.

[51] A. E. Lefohn, S. Sengupta, J. Kniss, R. Strzodka, and J. D. Owens. Glift: Generic, efficient, random-access gpu data structures. *ACM Trans. Graph.*, 25(1):60–99, 2006.

[52] J. Lengyel, M. Reichert, B. R. Donald, and D. P. Greenberg. Real-time robot motion planning using rasterizing computer graphics hardware. *SIGGRAPH Comput. Graph.*, 24(4):327–335, 1990.

[53] V. I. Levenshtein. Binary codes capable of correcting deletions, insertions and reversals. *Soviet Physics Doklady*, 10:707+, February 1966.

[54] A. Levinthal and T. Porter. Chap - a simd graphics processor. In *SIGGRAPH '84: Proceedings of the 11th annual conference on Computer graphics and interactive techniques*, pages 77–82, New York, NY, USA, 1984. ACM.

[55] K. I. Lin, H. V. Jagadish, and C. Faloutsos. The tv-tree: an index structure for high-dimensional data. *The VLDB Journal*, 3(4):517–542, October 1994.

[56] E. Lindholm, M. J. Kligard, and H. Moreton. A user-programmable vertex engine. In *SIGGRAPH '01: Proceedings of the 28th annual conference on Computer graphics and interactive techniques*, pages 149–158, New York, NY, USA, 2001. ACM.

[57] N. Linial, E. London, and Y. Rabinovich. The geometry of graphs and some of its algorithmic applications. *Combinatorica*, 15:215–245, 1995.

[58] X. Lu, Y. Wang, and A. K. Jain. Combining classifiers for face recognition. In *ICME '03: Proceedings of the 2003 International Conference on Multimedia and Expo - Volume 3 (ICME '03)*, pages 13–16, Washington, DC, USA, 2003. IEEE Computer Society.

[59] D. Maio and D. Maltoni. A structural approach to fingerprint classification. In *ICPR '96: Proceedings of the International Conference on Pattern Recognition (ICPR '96) Volume III-Volume 7276*, pages 578–585, Washington, DC, USA, 1996. IEEE Computer Society.

[60] D. Manocha. Quick-cullide: Fast inter- and intra-object collision culling using graphics hardware. In *VR '05: Proceedings of the 2005 IEEE Conference 2005 on Virtual Reality*, pages 59–66, 319, Washington, DC, USA, 2005. IEEE Computer Society.

[61] W. R. Mark, R. S. Glanville, K. Akeley, and M. J. Kilgard. Cg: a system for programming graphics hardware in a c-like language. In *SIGGRAPH '03: ACM SIGGRAPH 2003 Papers*, pages 896–907, New York, NY, USA, 2003. ACM.

[62] M. McCool, S. Du Toit, T. Popa, B. Chan, and K. Moule. Shader algebra. In *SIGGRAPH '04: ACM SIGGRAPH 2004 Papers*, pages 787–795, New York, NY, USA, 2004. ACM.

[63] P. McCormick, J. Inman, J. Ahrens, J. Mohd-Yusof, G. Roth, and S. Cummins. Scout: a data-parallel programming language for graphics processors. *Parallel Comput.*, 33(10-11):648–662, 2007.

[64] L. Mico, J. Oncina, and R. Carrasco. A fast branch-and-bound nearest-neighbor classifier in metric-spaces. 17(7):731–739, June 1996.

[65] L. Micó, J. Oncina, and E. Vidal. A new version of the nearest-neighbour approximating and eliminating search algorithm (aesa) with linear preprocessing time and memory requirements. *Pattern Recognition Letters*, 15(1):9–17, 1994.

[66] G. Navarro. Searching in metric spaces by spatial approximation. *The VLDB Journal*, 11:141–148, 1999.

[67] S. A. Nene and S. K. Nayar. A simple algorithm for nearest neighbor search in high dimensions. *IEEE Trans. Pattern Anal. Mach. Intell.*, 19(9):989–1003, 1997.

[68] M. Olano and A. Lastra. A shading language on graphics hardware: the pixelflow shading system. In *SIGGRAPH '98: Proceedings of the 25th annual conference on Computer graphics and interactive techniques*, pages 159–168, New York, NY, USA, 1998. ACM.

[69] Opengl, D. Shreiner, M. Woo, J. Neider, and T. Davis. *OpenGL(R) Programming Guide : The Official Guide to Learning OpenGL(R), Version 2 (5th Edition)*. Addison-Wesley Professional, August 2005.

[70] J. Owens. Streaming architectures and technology trends. In *SIGGRAPH '05: ACM SIGGRAPH 2005 Courses*, page 9, New York, NY, USA, 2005. ACM.

[71] J. D. Owens, D. Luebke, N. Govindaraju, M. Harris, J. Krüger, A. E. Lefohn, and T. J. Purcell. A survey of general-purpose computation on graphics hardware. *Computer Graphics Forum*, 26(1):80–113, March 2007.

[72] M. Pharr and R. Fernando. *GPU Gems 2: Programming Techniques for High-Performance Graphics and General-Purpose Computation*. Addison-Wesley Professional, March 2005.

[73] M. Potmesil and E. M. Hoffert. The pixel machine: a parallel image computer. *SIGGRAPH Comput. Graph.*, 23(3):69–78, 1989.

[74] T. Purcell and J. Sen. Shadesmith fragment program debugger., 2003.

[75] T. J. Purcell. *Ray tracing on a stream processor*. PhD thesis, Stanford, CA, USA, 2004. Adviser-Hanrahan, Patrick M.

[76] T. J. Purcell, C. Donner, M. Cammarano, H. W. Jensen, and P. Hanrahan. Photon mapping on programmable graphics hardware. In *SIGGRAPH '05: ACM SIGGRAPH 2005 Courses*, page 258, New York, NY, USA, 2005. ACM.

[77] H. Samet. *The design and analysis of spatial data structures*. Addison-Wesley Longman Publishing Co., Inc., Boston, MA, USA, 1990.

[78] H. Samet. Spatial data structures. In *Modern Database Systems: The Object Model, Interoperability, and Beyond.*, pages 361–385. 1995.

[79] T. Seidl and H. P. Kriegel. Optimal multi-step k-nearest neighbor search. In *SIGMOD Conference*, pages 154–165, 1998.

[80] R. Strzodka. Virtual 16 bit precise operations on RGBA8 textures. In *Proceedings of Vision, Modeling, and Visualization (VMV'02)*, pages 171–178, 2002.

[81] R. Strzodka and C. Garbe. Real-time motion estimation and visualization on graphics cards. In *VIS '04: Proceedings of the conference on Visualization '04*, pages 545–552, Washington, DC, USA, 2004. IEEE Computer Society.

[82] D. Tarditi, S. Puri, and J. Oglesby. Accelerator: using data parallelism to program gpus for general-purpose uses. *SIGARCH Comput. Archit. News*, 34(5):325–335, 2006.

[83] D. Trebilco. Glintercept. Available at `http://glintercept.nutty.org/`, 2006.

[84] C. Trendall and A. J. Stewart. General calculations using graphics hardware with applications to interactive caustics. In *Proceedings of the Eurographics Workshop on Rendering Techniques 2000*, pages 287–298, London, UK, 2000. Springer-Verlag.

[85] J. K. Uhlmann. Satisfying general proximity/similarity queries with metric trees. *Information Processing Letters*, 40(4):175–179, 1991.

[86] S. Upstill. *RenderMan Companion: A Programmer's Guide to Realistic Computer Graphics*. Addison-Wesley Longman Publishing Co., Inc., Boston, MA, USA, 1989.

[87] E. Vidal Ruiz. An algorithm for finding nearest neighbors in (approximately) constant time. 4:145–157, 1986.

[88] J. T.-L. Wang and D. Shasha. Query processing for distance metrics. In *VLDB '90: Proceedings of the 16th International Conference on Very Large Data Bases*, pages 602–613, San Francisco, CA, USA, 1990. Morgan Kaufmann Publishers Inc.

[89] J. T.-L. Wang, X. Wang, K.-I. Lin, D. Shasha, B. A. Shapiro, and K. Zhang. Evaluating a class of distance-mapping algorithms for data mining and clustering. In *KDD*, pages 307–311, 1999.

[90] D. A. White and R. Jain. Similarity indexing with the ss-tree. In *ICDE '96: Proceedings of the Twelfth International Conference on Data Engineering*, pages 516–523, Washington, DC, USA, 1996. IEEE Computer Society.

[91] J. Woetzel and R. Koch. Multi-camera real-time depth estimation with discontinuity handling on pc graphics hardware. In *ICPR '04: Proceedings of the Pattern Recognition, 17th International Conference on (ICPR'04) Volume 1*, pages 741–744, Washington, DC, USA, 2004. IEEE Computer Society.

[92] R. Yang and M. Pollefeys. A versatile stereo implementation on commodity graphics hardware. *Real-Time Imaging*, 11(1):7–18, 2005.

[93] P. N. Yianilos. Data structures and algorithms for nearest neighbor search in general metric spaces. In *SODA '93: Proceedings of the fourth annual ACM-SIAM Symposium on Discrete algorithms*, pages 311–321, Philadelphia, PA, USA, 1993. Society for Industrial and Applied Mathematics.

[94] S.-E. Yoon, P. Lindstrom, V. Pascucci, and D. Manocha. Cache-oblivious mesh layouts. In *SIGGRAPH '05: ACM SIGGRAPH 2005 Papers*, pages 886–893, New York, NY, USA, 2005. ACM.